$CHCH_3$), 1.99 (t, 1 H, C≡C*H*), 2.41 (dd, 2 H, CH_2CH), 3.33 (dt, 1 H, $CHOCH_2CF_3$), 3.87, 4.03 (2dq, 2 H, CH_2CF_3); GC/MS, *m/e* 194 (1%, M^+), 179 (8), 155 (100%, $M^+ - C_3H_3$).

4-Isopropyl-1-(2,2,2-trifluoroethoxy)cyclobutene (66): ^1H NMR ($CDCl_3$, 400 MHz) δ 0.87, 0.94 (2d, 6 H, isopropyl-CH_3), 1.68 (m, 1 H, isopropyl-CH), 2.09 (dd, 1 H, part of CH_2), 2.73 (m, 1 H, ring CH), 3.47 (br s, 1 H, part of CH_2), 4.06 (q, 2 H, CH_2CF_3), 4.58 (br s, 1 H, C=C*H*); GC/MS, *m/e* 194 (23%, M^+), 179 (100%, $M^+ - CH_3$).

4-Methyl-5-(2,2,2-trifluoroethoxy)-1-hexyne (68, Two Diastereomers): ^1H NMR ($CDCl_3$, 400 MHz) δ 0.98/1.00 (d, 3 H, CH_3), 1.14/1.15 (d, 3 H, CH_3), 1.76-1.86/1.73-1.83 (m, 1 H, 4-H), 1.939/1.942 (t, 1 H, 1-H), 2.27, 2.38/2.11, 2.33 (2m and 2ddd, 2 H, CH_2), 3.46/3.61 (m, 1 H, 5-H), 3.7-3.9 (m, 2 H, CH_2CF_3); GC/MS, *m/e* 194 (1%, M^+), 127 (100%, $M^+ - C_5H_7$), 179 (10).

4-Methyl-4-(2,2,2-trifluoroethoxy)-1-hexyne (69): ^1H NMR ($CDCl_3$, 400 MHz) δ 0.89 (t, 3 H, CH_2CH_3), 1.26 (s, 3 H, CCH_3), 1.61, 1.66 (2dq, 1 H each, $CHCH_3$), 2.00 (t, 1 H, C≡C*H*), 2.28, 2.38 (m, 2 H, CHC≡CH), 3.7-3.9 (m, 2 H, CH_2CF_3); GC/MS, *m/e* 194 (M^+, not found), 179 (17), 165 (42%, $M^+ - C_2H_5$), 155 (100%, $M^+ - C_3H_3$).

5-Methyl-5-(2,2,2-trifluoroethoxy)-1-hexyne (70): ^1H NMR ($CDCl_3$, 400 MHz) δ 1.19 (s, 6 H, 2 × CH_3), 1.66-1.84 (m, 2 H, 4-H), 1.91 (t, 1 H, C≡C*H*), 2.09-2.28 (m, 2 H, 3-H), 3.68 (q, 2 H, CH_2CF_3), GC/MS, *m/e* 194 (1%, M^+) 179 (27), 141 (100%, $M^+ - C_4H_5$).

2,3-Dimethyl-1 (2,2,2-trifluoroethoxy)cyclobutene (51): ^1H NMR ($CDCl_3$, 400 MHz) δ 1.05 (d, 3 H, 3-CH_3), 1.58 (m, 3 H, 2-CH_3), 1.96 (m, 1 H, part of CH_2), 2.23 (m, 1 H, C*H*-CH_3), 2.77 (m, 1 H, part of CH_2) 4.13 (q, 2 H, CH_2CF_3), GC/MS, *m/e* 180 (100%, M^+), 165 (73), 140 (7), 127 (13).

2,4-Dimethyl-1-(2,2,2-trifluoroethoxy)cyclobutene (53): ^1H NMR ($CDCl_3$, 400 MHz) δ 1.13 (d, 3 H, 4-CH_3), 1.47 (m, 1 H, part of CH_2), 1.66 (m, 3 H, 2-CH_3), 2.14 (m, 1 H, part of CH_2), 2.82 (m, 1 H, $CHCH_3$), 4.20 (2dq, 2 H, CH_2CF_3); GC/MS, *m/e* 180 (90%, M^+), 179 (43), 185 (90), 67 (100).

5-(2,2,2-Trifluoroethoxy)-2-hexyne (55): ^1H NMR ($CDCl_3$, 400 MHz) δ 1.27 (d, 3 H, $CHCH_3$), 1.77 (t, 3 H, $CCCH_3$), 2.22-2.33 and 2.36-2.47 (2m, 1 H each, CH_2), 3.67 (tq, 1 H, $CHCH_3$), 3.87 (2dq, 2 H, CH_2CF_3); GC/MS, *m/e* 180 (37%, M^+), 165 (33), 127 (100%, $M^+ - C_4H_5$).

8-(2,2,2-Trifluoroethoxy)bicyclo[4.2.0]oct-1(8)-ene (75): ^1H NMR ($CDCl_3$, 400 MHz) δ 0.86-1.00 (m, 1 H), 1.15-1.20 (m, 2 H), 1.65-1.78 (m, 2 H), 1.80-1.90 (m, 1 H), 1.90-2.04 (m, 2 H), 2.14, 2.37 (2dd, 1 H each, 4-ring-CH_2), 2.64 (dt, 1 H, bridgehead-CH), 4.17 (q, 2 H, CH_2CF_3); GC/MS, *m/e* 206 (57%, M^+), 191 (35), 177 (30), 165 (10), 152 (2), 127 (16), 107 (30), 91 (57), 79 (71), 43 (100).

10-(2,2,2-Trifluoroethoxy)bicyclo[6.2.0]dec-1(10)-ene (77): GC/MS, *m/e* 234 (M^+, absent), 219 (10), 206 (12), 205 (13), 193 (13), 191 (33), 178 (14), 177 (13), 165 (100), 153 (14), 152 (16), 139 (57).

6-(2,2,2-Trifluoroethoxy)bicyclo[3.2.0]hept-6-ene (83): ^1H NMR ($CDCl_3$) δ 0.75-1.80 (m, ring-CH_2), 2.77 (m, 1 H, CHCO), 3.23 (m, 1 H, CHC=C), 4.05 (q, 2 H, CH_2CF_3), 4.43 (br s, C=C*H*); GC/MS, *m/e* 192 (59%, M^+), 177 (100), 164 (39), 109 (34), 93 (43), 91 (38), 81 (63).

***trans*-2-Ethynyl-1-(2,2,2-trifluoroethoxy)cyclopentane (84)**: GC/MS, *m/e* 192 (M^+, absent), 191 (32%, $M^+ - H$), 177 (24), 152 (46), 139 (61), 93 (88), 91 (100).

7-(2,2,2-Trifluoroethoxy)bicyclo[4.2.0]oct-7-ene (88): GC/MS, *m/e* 206 (9%, M^+), 191 (15), 178 (13), 177 (55), 165 (10), 164 (6), 67 (100).

***trans*-2-Ethynyl-1-(2,2,2-trifluoroethoxy)cyclohexane (89)**: GC/MS, *m/e* 206 (M^+, absent), 191 (29), 178 (27), 177 (23), 165 (28), 139 (100).

9-(2,2,2-Trifluoroethoxy)bicyclo[4.2.0]oct-7-ene (90): GC/MS, *m/e* 234 (13%, M^+), 219 (10, 205 (15), 192 (35), 191 (72), 180 (49), 177 (88), 67 (100).

***trans*-2-Ethynyl-1-(2,2,2-trifluoroethoxy)cyclooctane (91)**: GC/MS, *m/e* 234 (M^+, absent), 233 (2), 205 (7), 191 (25), 165 (61), 139 (49), 91 (85), 79 (100).

Acknowledgment. We thank the Fonds der Chemischen Industrie for financial support and Prof. C. J. Collins, Department of Chemistry, University of Tennessee, for carefully going through the manuscript.

Ground Term Splitting of High-Spin Co^{2+} as a Probe of Coordination Structure. 1. Dependence of the Splitting on Coordination Geometry[1a]

Marvin W. Makinen,*[1b] Lawrence C. Kuo,[1c] Moon B. Yim, Gregg B. Wells,[1d] James M. Fukuyama, and Judy E. Kim

Contribution from the Department of Biophysics and Theoretical Biology, The University of Chicago, Cummings Life Science Center, Chicago, Illinois 60637. *Received April 9, 1984*

Abstract: The sign and magnitude of the splitting between the two lowest Kramers doublets (Δ) of high-spin Co^{2+} in a variety of structurally defined, small molecule coordination complexes is determined. The range of values of Δ is found to be <13 cm^{-1} in tetracoordinate sites, ~20-50 cm^{-1} in pentacoordinate sites of trigonal-bipyramidal or square-pyramidal geometry, and ≥50 cm^{-1} in hexacoordinate sites. It is shown on the basis of group theoretical arguments and estimates of the zero-field splitting derived by second-order perturbation theory that the observed range of values of Δ correlates well with that predicted by theory. On this basis, it is suggested that the splitting between the two lowest Kramers doublets of high-spin Co^{2+} may provide a diagnostic signature of coordination geometry.

Except for diffraction techniques, there are no methods to determine directly the structure of metal ion coordination complexes. This circumstance is particularly true upon substitution of metal ions into metalloproteins and enzymes as spectroscopic probes, for evaluation of the coordination environment generally rests heavily on the assumption that the metal ion binding site remains isostructural with that defined by X-ray crystallographic studies of the native enzyme. High-spin Co^{2+} has been employed as a spectroscopic probe of Zn^{2+} metalloenzymes since it usually can be incorporated into the apoenzyme to regenerate catalytic activity.[2] However, the spectroscopic complexities of high-spin Co^{2+} with respect to the orbital degeneracy of the ground state and coupling of excited state terms with changes in coordination environment have resulted only in qualitative characterization of

(1) (a) This work was supported by NIH Grant GM 21900. (b) Established Investigator of The American Heart Association for part of the tenure of this investigation. (c) Predoctoral student supported by a training grant of the NIH (GM 07183). Present address: Department of Chemistry, Boston University, Boston, MA 02215. (d) Predoctoral student supported by an MSTP grant of the NIH (GM 07281).

(2) (a) Lindskog, S. *Struct. Bonding (Berlin)* **1970**, *8*, 153-196. (b) Makinen, M. W. In "Techniques and Topics in Bioinorganic Chemistry"; MacAuliffe, C. A., Ed.; MacMillan: London **1975**; pp 3-106. (c) Bertini, I.; Luchinat, C. *Acc. Chem. Res.* **1983**, *16*, 272-279.

0002-7863/85/1507-5245$01.50/0

metal ion binding sites in enzymes by electron paramagnetic resonance methods. For these reasons, high-spin Co^{2+} has been employed primarily as an optical probe of metalloproteins to measure ionization and equilibrium binding constants and to monitor kinetic events.[2,3]

The splitting of spectroscopic states of high-spin Co^{2+} in coordination complexes results in two general patterns due to the combined effects of the symmetry of the crystal field and spin–orbit coupling.[4] They correspond to a high-spin d^7 configuration either in an orbitally nondegenerate ground state ($^4A_2$) or in an orbitally degenerate ground state ($^4T_1$) in which the orbital levels are separated by spin–orbit coupling. In the case of an orbitally nondegenerate ground state, as may be found in tetra- and pentacoordinate sites, the orbital angular momentum is quenched and the combined effects of crystal field symmetry and admixture of excited terms through second-order spin–orbit coupling may lead to a splitting of the two Kramers doublets ($m_s = \pm^1/_2, \pm^3/_2$) of the $^4A_2$ ground-state term in the absence of an applied magnetic field. This is known as the zero-field splitting and is defined in the spin Hamiltonian as $\mathbf{S}\cdot\mathbf{D}\cdot\mathbf{S}$ where $\mathbf{S}$ is the spin angular momentum and $\mathbf{D}$ is the zero-field splitting tensor. On the other hand, with an orbitally degenerate ground state, the levels are split by the spin–orbit coupling, and, in general, the combined effects of spin–orbit coupling and distortion of the crystal field from high symmetry lead to a series of Kramers doublets. In this case the $^4T_1$ ground state is split into a series of levels approximately described by a fictitious orbital angular momentum $L = 1$ and corresponding J values of $^1/_2$ ($m_J = \pm^1/_2$), $^3/_2$ ($m_J = \pm^3/_2, \pm^1/_2$), and $^5/_2$ ($m_J = \pm^5/_2, \pm^3/_2, \pm^1/_2$).

To develop a method of assigning the coordination geometry and structural environment of high-spin Co^{2+} substitutionally incorporated into metalloproteins, we have carried out a detailed analysis of the electron paramagnetic resonance properties of high-spin Co^{2+} in structurally defined sites. In the course of these investigations, we have observed that estimates of the splitting between the two lowest Kramers doublets can be conveniently determined with a conventional EPR[5] spectrometer by application of the cw microwave power saturation technique[6] that we have employed earlier in the study of hemeproteins. Through these investigations we have observed that there is a direct correlation of the value of the splitting with coordination structure. Here we demonstrate on the basis of results for structurally defined, small molecule complexes that the splitting (Δ) between the two lowest Kramers doublets of high-spin Co^{2+} follows the order

$$\Delta_4 < \Delta_5 \leq \Delta_6 \quad (1)$$

where the subscript designates the coordination geometry characteristic of classical tetra-, penta-, and hexacoordinate sites with monoatom donor ligands. We support this correlation on the basis of a group theoretical treatment of spin–orbit coupling and on the basis of relationships derived through second-order perturbation theory to show that the predicted range of values of Δ corresponds closely to that determined spectroscopically.

Experimental Procedures

Materials. Cobalt metal rod (Specpur) was obtained from Johnson-Matthey and dissolved in Baker Ultrex HCl. Anhydrous $CoCl_2$ was obtained from this solution by removal of solvent in vacuo. Organic compounds employed as ligands were of the highest purity commercially available and were recrystallized several times prior to use according to methods reported in the corresponding cited synthesis procedures. The ligand $MePh_2AsO$ was prepared by reaction of $MePh_2As$ (Alfa Products, Danvers, MA) with $KMnO_4$ and recrystallized[7] until colorless (mp 152–153 °C (obsd), 153–155 °C (lit.)). The solid product yielded no spurious paramagnetic signals. Elemental analysis showed (calculated) 60.04% C, 5.00% H, 28.81% As; found 59.98% C, 4.86% H, 28.93% As. The analogous compound $MePh_2PO$ obtained from Alfa Products was recrystallized several times from benzene before use.

Polycrystalline $Co_{0.001}Zn_{0.999}(imidazole)_2(acetate)_2$,[8] $Co_{0.001}Zn_{0.999}(Ph_3PO)_2Cl_2$,[9,10] $Co_{0.001}Zn_{0.999}(2\text{-picoline } N\text{-oxide})_5(ClO_4)_2$,[11,12] $Co_{0.0002}Mg_{0.9998}(acetate)_2\cdot 4H_2O$,[13,14] $Co_{0.0005}Zn_{0.9995}SO_4\cdot 7H_2O$,[15,16] $Co_{0.002}Zn_{0.998}(MePh_2AsO)_4(ClO_4)_2$,[17,18] and $Co_{0.002}Zn_{0.998}(Ph_3P)_2Cl_2$[19,20] were prepared by cocrystallization according to the cited procedures. In general, Johnson-Matthey Puratronic grade materials were employed wherever possible. The concentration of Co^{2+} is given for that in solution from which crystals were grown. In each case the highest concentration of Co^{2+} was employed that did not induce near-neighbor, magnetic interactions that perturbed the relaxation or spectral properties of the Co^{2+} ion in these polycrystalline complexes. The complex $Co(Me_2SO)_6(ClO_4)_2$[21,22] was prepared by dissolving Johnson-Matthey (Puratronic) $Co(ClO_4)_2$ in vacuum distilled, neat (Baker) Me_2SO because sufficiently high concentrations of Co^{2+} in crystals of the host isomorphous $Zn(Me_2SO)_6(ClO_4)_2$ complex could not be obtained for data collection under conditions of sufficiently high signal-to-noise ratios without interference from magnetic site–site interactions. In neat Me_2SO the Co^{2+} ion is coordinated to six Me_2SO molecules as in the crystal.[22] For similar reasons, the hexacoordinate complex Co(pyridine N-oxide)$_6(ClO_4)_2$[23,24] was prepared by dissolving Johnson-Matthey Puratronic $Co(ClO_4)_2$ with an approximate 2-fold excess of the ligand in distilled water. Complexes of $Co(MePh_2PO)_4(ClO_4)_2$, $Co(MePh_2AsO)_4(ClO_4)_2$,[17,18] and $Co(Ph_3P)_2Cl_2$[19,20] were also prepared by addition of $Co(ClO_4)_2$ or $CoCl_2$ to the ligand in absolute ethanol. Solutions of these complexes were frozen directly in EPR sample tubes for spectroscopic studies.

Two complexes of high-spin Co^{2+} were investigated because of their known, large, negative values of D. The complex Cs_3CoBr_5 was prepared by dissolving cobalt metal bar in Johnson-Matthey Puratronic HBr, followed by solvent removal in vacuo. The anhydrous salt was then redissolved in an aqueous solution of CsBr under the conditions that are employed to crystallize the salt from aqueous solution.[25] This complex was studied in frozen solution only since crystals of pure Cs_3CoBr_5 cannot be used for cw power saturation studies and cocrystallization of $CoBr_2$ or $CoCl_2$ with the corresponding zinc compound results only in crystals of $Cs_2Zn(Co)X_4$. The value of $2D$ of high-spin Co^{2+} incorporated into the latter crystal is large and positive.[26,27] We have also compared the value of Δ determined for samples of polycrystalline $Co_{0.002}Zn_{0.998}(Ph_3P)_2Cl_2$ with that of the Co^{2+} complex prepared in absolute ethanol, from which solvent crystals were prepared for spectroscopic studies by others.[20] The value of D for the Co^{2+} in pure single crystals of Co-

(3) (a) Coleman, J. E.; Vallee, B. L. *J. Biol. Chem.* **1960**, *235*, 390–395. (b) Coleman, J. E.; Vallee, B. L. *J. Biol. Chem.* **1961**, *236*, 2244–2249. (c) Latt, S. A.; Vallee, B. L. *Biochemistry* **1971**, *10*, 4263–4270. (d) Kennedy, F. S.; Hill, H. A. O.; Kaden, T. A.; Vallee, B. L. *Biochem. Biophys. Res. Commun.* **1972**, *48*, 1533–1539.

(4) Carlin, R. L.; von Duyneveldt, A. J. "Magnetic Properties of Transition Metal Compounds"; Springer Verlag: New York, 1977; Chapter 1, pp 1–22.

(5) The following abbreviations are used: cw continuous wave; Me_2SO, dimethyl sulfoxide; EPR, electron paramagnetic resonnce; Me, methyl; Ph, phenyl; zfs, zero field splitting; the symbol Δ is used to designate the separation between the two lowest Kramers doublets of high-spin Co^{2+}; in the case of high-spin Co^{2+} with a nondegenerate ground state, it is identical with the zfs.

(6) Yim, M. B.; Kuo, L. C.; Makinen, M. W. *J. Magn. Reson.* **1982**, *46*, 247–256.

(7) Blicke, F. F.; Safir, S. R. *J. Am. Chem. Soc.* **1941**, *63*, 575–576.

(8) Horrocks, W. DeW., Jr.; Ishley, J. N.; Holmquist, B.; Thompson, J. S. *J. Inorg. Biochem.* **1980**, *12*, 131–141.

(9) (a) Vivien, D.; Gibson, J. F. *J. Chem. Soc., Faraday Trans. 2* **1975**, *71*, 1640–1653. (b) Bertrand, J. A.; Kalyanaraman, A. R. *Inorg. Chim. Acta* **1971**, *5*, 341–345.

(10) Goodgame, D. M. L.; Cotton, F. A. *J. Chem. Soc. A* **1961**, 3735–3741.

(11) Coyle, B. A.; Ibers, J. A. *Inorg. Chem.* **1970**, *9*, 767–772.

(12) Byers, W.; Lever, A. B. P.; Parish, R. V. *Inorg. Chem.* **1968**, *7*, 1835–1840.

(13) van Niekerk, J. N.; Schoening, F. R. L. *Acta Crystallogr.* **1953**, *6*, 609–612.

(14) Lowrey, M. R.; Pilbrow, J. R. *J. Magn. Reson.* **1979**, *34*, 103–112.

(15) Fritz, J. J.; Giauque, W. F. *J. Am. Chem. Soc.* **1949**, *71*, 2168–2176.

(16) Bleaney, B.; Ingram, D. J. E. *Proc. R. Soc. London, Ser. A.* **1951**, *208*, 143–158.

(17) Lewis, J.; Nyholm, R. S.; Rodley, G. A. *Nature (London)* **1965**, *207*, 72–73.

(18) Pauling, P.; Robertson, G. B.; Rodley, G. A. *Nature (London)* **1965**, *207*, 73–74.

(19) Carlin, R. L.; Chirico, R. D.; Sinn, E.; Mennenga, G.; De Jongh, L. J. *Inorg. Chem.* **1982**, *21*, 2218–2222.

(20) Simo, C.; Holt, S. *Inorg. Chem.* **1968**, *7*, 2655–2657.

(21) Currier, W. F.; Weber, J. H. *Inorg. Chem.* **1967**, *6*, 1539–1543.

(22) Persson, I. *Acta Chem. Scand., Ser A* **1982**, *A36*, 7–13.

(23) Carlin, R. L.; O'Connor, C. J.; Bhatia, S. N. *J. Am. Chem. Soc.* **1976**, *98*, 685–688.

(24) (a) Bergendahl, T. J.; Wood, J. S. *Inorg. Chem.* **1975**, *14*, 338–342. (b) van Ingen Schenau, A. D.; Verschoor, G. C.; Romers, C. *Acta Crystallogr., Sect. B* **1974**, *B30*, 1686–1694.

(25) van Stapele, R. P.; Beljers, H. G.; Bongers, P. F.; Zijlstra, H. *J. Chem. Phys.* **1966**, *44*, 3719–3725.

(26) McElearney, J. N.; Merchant, S.; Shankle, G. E.; Carlin, R. L. *J. Chem. Phys.* **1977**, *66*, 450–458.

(27) Blöte, H. W. J.; Huiskamp, W. J. *Physica* **1971**, *53*, 445–470.

$(Ph_3P)_2Cl_2$ is reported as large and negative.[19] We have compared these results to that obtained by dissolving in absolute ethanol a large single crystal of $Co(Ph_3P)_2Cl_2$ provided by Professor R. L. Carlin of the Department of Chemistry at the University of Illinois at Chicago.

We have extensively surveyed the literature (reviewed in ref 28) for other structurally defined complexes of high-spin Co^{2+} suitable for these spectroscopic studies. Except for the complexes presented here, two factors have invariably prevented extension of our studies to the variety of potentially suitable compounds: (i) the spin–lattice relaxation rates remain much too fast in the 4–12 K range for adequate microwave power saturation of the EPR transitions to determine the value of Δ or (ii) it has not always been feasible to prepare materials totally devoid of extraneous paramagnetic impurities that perturb the temperature dependence of the spin–lattice relaxation of the Co^{2+} sites. Unfortunately this has been true also in our attempts to prepare the classical pentacoordinate complexes $Zn(Co)[(HN(CH_2CH_2N(C_2H_5)_2]_2Cl_2$,[29,30] $Zn(Co)$(terpyridyl)Cl_2,[31] and $Zn(Co)[N(CH_2CH_2N(CH_3)_2]_3Br_2$[32] in suitable polycrystalline form with complete absence of perturbing, contaminant, paramagnetic species. Moreover, the Co^{2+} complexes in ethanolic solution exhibited spin–lattice relaxation rates too fast for adequate microwave power saturation to determine the value of Δ by the cw power saturation technique[6] employed in this investigation.

Methods. EPR spectra were recorded with an X-band Bruker ER200D spectrometer operated at 100-kHz frequency modulation in the TE_{102} mode. The spectrometer was equipped with an Oxford Instruments ESR10 liquid helium cryostat.[33] The microwave power incident on the cavity was calibrated with a Hewlett-Packard 436A power meter in the 0.1–640-mW range. The temperature of the sample in the cavity was determined with a gold chromel thermocouple or carbon resistor thermometer in the 3–20 K range according to the calibration method previously described.[6] We have established that this procedure yields a reproducibility of ±0.3 K in defining the sample temperature when the helium flow rate is adjusted so that at the lowest temperature achievable with this cryostat a stable diode current is observed at 0 dB (640 mW) of microwave power attenuation.

The cw microwave power saturation technique developed in this laboratory[6] was employed for estimating the splitting between the two lowest Kramers doublets of high-spin Co^{2+} in polycrystalline materials and in coordination complexes in frozen solutions. We have previously observed[34–36] that the reproducibility in applying this technique to estimate the value of the parameter log $P_{1/2}$ from progressive microwave power saturation curves and the value of Δ from the temperature dependence of log $P_{1/2}$ is ±10%. The results reported in this study are based on measurements of at least two independently prepared samples. In general, such samples yielded good agreement (to within ±10%) in the determination of Δ. Since we were constrained by costs for the expenditure of liquid helium, measurements of $P_{1/2}$ with the second and subsequent samples were made over larger temperature intervals essentially only to confirm the value of Δ and to ensure accurate identification of the temperature range in which the mechanism of spin–lattice relaxation corresponds predominantly to the Orbach process.[37–39]

Comparison of the magnitude of Δ measured by spin–lattice relaxation techniques, e.g., pulse saturation and recovery, shows that the agreement is within ±15% of that determined by, for instance, infrared optical techniques.[40] The difference arises from a distribution of values of Δ throughout a given sample, but this distribution remains within 2 standard deviations of the measurement. In preliminary studies, we have observed that values of the zfs constants of high-spin Fe^{3+} complexes of hemeproteins determined by application of this cw saturation technique agree to within ±10% of those determined by magnetic susceptibility methods.[6] Since the reproducibility of measured values of Δ is ±10% by the cw power saturation technique,[6,34–36] we conclude that these measurements are determined as accurately as by application of pulse saturation and recovery methods.

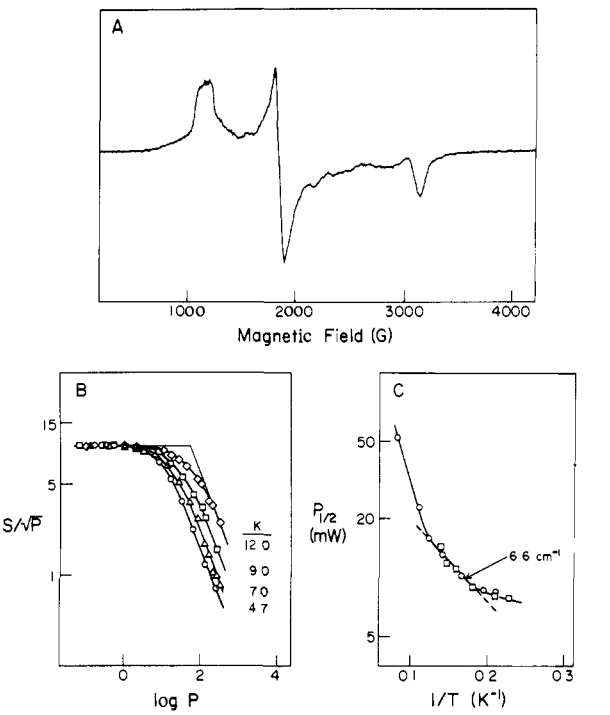

Figure 1. First-derivative EPR absorption spectrum and cw microwave power saturation properties of bis(triphenylphosphine oxide)cobalt(II) dichloride incorporated to ≤0.1 mol % into the polycrystalline matrix of the Zn^{2+} complex. (A) illustrates the spectrum recorded with the sample at 4.7 K and under conditions of 0.66-mW incident microwave power and 10-G amplitude modulation. Resonance features appear at g values of ~5.91, 3.64, and 2.15. In the low-field region hyperfine structure due to the ($I = {}^7/_2$) ^{59}Co nucleus is resolved, indicating an (average) hyperfine coupling constant of 0.0055 cm^{-1}. This is comparable to that observed in other tetracoordinate complexes of high-spin Co^{2+}.[28,42] (B) illustrates the cw power saturation behavior of the $g \sim 3.64$ component at 4.7, 7.0, 9.0, and 12 K. The data show that the value of b (−1.50) at high power levels remains temperature invariant over the 4–12 K range. (C) illustrates the temperature dependence of $P_{1/2}$ estimated by the cw saturation method[6] for two different polycrystalline samples, illustrated by circles and squares, respectively. Although the absolute $P_{1/2}$ values differ for the two samples because of different sample volumes, the $P_{1/2}$ data of one set have been frame-shifted to coincide with those of the second sample. The linear region in the 4.7–8.0 K range yields an estimate of 6.6 cm^{-1} for the value of Δ. For preparation of this polycrystalline complex, Johnson-Matthey (Puratronic) ZnO was dissolved in Baker Ultrex HCl and the solution was evaporated to dryness. Both the Co^{2+} and Zn^{2+} salts were then prepared and cocrystallized[8,9] from absolute ethanol.

Results

A. Tetracoordinate Complexes of High-Spin Co^{2+}. To determine the splitting between the two lowest Kramers doublets of high-spin paramagnetic metal ions, the signal amplitude of a suitable resonance line of the paramagnetic species is monitored as a function of incident microwave power and temperature. This procedure is illustrated in Figure 1 for polycrystalline $Co_{0.001}Zn_{0.999}(Ph_3PO)_2Cl_2$. In Figure 1A the spectrum is identical with that reported by Bencini et al.[41] Figure 1B illustrates representative progressive microwave power saturation curves for the peak-to-peak amplitude of the $g \sim 3.64$ resonance band. The data are plotted in a form[43–45] that yields a graphical estimate

(28) Banci, L., Bencini, A.; Benelli, C.; Gatteschi, D.; Zanchini, C. *Struct. Bonding (Berlin)* **1982**, *52*, 37–86.
(29) Dori, Z.; Eisenberg, R.; Gray, H. B. *Inorg. Chem.* **1967**, *6*, 483–486.
(30) Dori, Z.; Gray, H. B. *Inorg. Chem.* **1968**, *7*, 889–892.
(31) (a) Einstein, F. W. B.; Penfold, B. R. *Acta Crystallogr.* **1966**, *20*, 924–926. (b) Goldschmied, E.; Stephenson, N. C. *Acta Crystallog. Sect. B* **1970**, *B26*, 1867–1875.
(32) Di Vaira, M.; Orioli, P. L. *Inorg. Chem.* **1967**, *6*, 955–957.
(33) Campbell, S. J.; Herbert, I. R.; Warnick, C. B.; Woodgate, J. M. *Rev. Sci. Instrum.* **1976**, *47*, 1172–1176.
(34) Kuo, L. C.; Makinen, M. W. *J. Biol. Chem.* **1982**, *257*, 24–27.
(35) Makinen, M. W.; Yim, M. B. *Proc. Natl. Acad. Sci. U.S.A.* **1981**, *78*, 6221–6225.
(36) Makinen, M. W.; Maret, W.; Yim, M. B. *Proc. Natl. Acad. Sci. U.S.A.* **1983**, *80*, 2584–2588.
(37) Orbach, R. *Proc. R. Soc. London, Ser. A* **1961**, *264A*, 485–495.
(38) Finn, C. B. P.; Orbach, R.; Wolf, W. P. *Proc. Phys. Soc., London* **1961**, *77*, 261–268.
(39) Orbach, R.; Stapleton, H. J. In "Electron Paramagnetic Resonance"; Geschwind, S., Ed.; Plenum Press: New York, 1972; Chapter 2, pp 121–216.
(40) Young, B. A.; Stapleton, H. J. *Phys. Rev.* **1968**, *176*, 502–509.
(41) Bencini, A.; Benelli, C.; Gatteschi, D.; Zanchini, C. *Inorg. Chem.* **1979**, *18*, 2137–2140.
(42) McGarvey, B. R. In "Transition Metal Chemistry"; Carlin, R. L., Ed.; Marcel Dekker: New York, 1966; Vol. 3, pp 89–201.
(43) Beinert, H.; Orme-Johnson, W. H. In "Magnetic Resonance in Biological Systems"; Ehrenberg, A., Malmström, B., Vänngard, T., Eds.; Pergamon Press: Oxford, **1969**; pp 221–247.

of $P_{1/2}$ according to the relationship

$$S/P^{1/2} \propto (1 + P/P_{1/2})^{-b/2} \quad (2)$$

The parameter S is the normalized signal amplitude, P is the incident microwave power, b is a constant characteristic of the broadening mechanism and is a measure of the ratio of the spin-packet line width to the total line width of the (unsaturated) inhomogeneously broadened line envelope, and $P_{1/2}$ is the microwave power at which the value of the saturation factor $(1 + \gamma^2 H_1^2 T_1 T_2)^{-1}$ is 0.5. Here T_1 is the spin–lattice relaxation time, and T_2 is the spin–spin relaxation time that determines the spin-packet line width. The parameter $P_{1/2}$ is determined graphically from the intersection of the two asymptotes of the saturation curve.

For the family of saturation curves in Figure 1B, the value of the parameter b remained temperature invariant in the 4–12 K range, as did the line width of the $g \sim 3.64$ resonance feature. This observation requires that T_2 remains constant in this temperature range.[6] Since the parameter $P_{1/2}$ is defined by eq 3

$$P_{1/2} \propto 1/\gamma^2 T_1 T_2 \quad (3)$$

$P_{1/2}$ then varies according to the temperature dependence of the spin–lattice relaxation time.[46] These characteristics apply, furthermore, to all of the complexes of high-spin Co^{2+} presented in this study and, therefore, will not be individually discussed further.

In Figure 1C we have plotted the temperature dependence of $P_{1/2}$ for two different samples of polycrystalline $Co_{0.001}Zn_{0.999}(Ph_3PO)_2Cl_2$. The central region of the plot shows an approximately linear region corresponding to an exponential dependence of $P_{1/2}$ on $1/T$, while at high temperatures there is a sharp increase in slope for $T \geq 10$ K. On the basis of our previous studies,[6] we conclude that the $P_{1/2}$ data in the central region correspond to spin–lattice relaxation via the two-phonon Orbach process[37-39] while the high-temperature data reflect the gradual change in the mechanism of spin–lattice relaxation from the Orbach process to the multiphonon Raman process.[48] Saturation experiments at $T < 5$ K indicate that there is a gradual decrease in slope. By comparing the dependence of $P_{1/2}$ on temperature at $T < 5$ K with the temperature dependence of $1/T_1$ determined by pulse saturation and recovery techniques,[49] we have observed that phonon–spin coupling properties of the matrix become important in the low-temperature region in cw microwave saturation experiments and relaxation is dominated by spectral diffusion processes.[50]

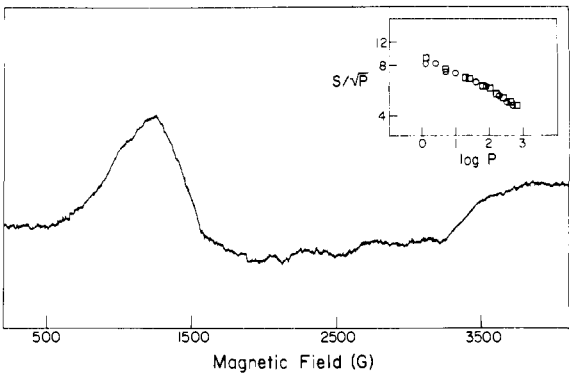

Figure 2. First-derivative EPR absorption spectrum and cw microwave power saturation properties of polycrystalline $Co_{0.002}Zn_{0.998}(Ph_3P)_2Cl_2$. The spectrum was recorded with the sample at 3.6 K with 20-mW incident microwave power and 12.5 G-amplitude modulation. The inset illustrates the cw microwave power saturation behavior of the low-field resonance feature at two different temperatures (○, 8 K; □, 10 K). The resonance features appear at g values of $\sim$ 4.6 and 2.2.

This circumstance prevents modeling of $P_{1/2}$ data at $T < 5$ K, and, therefore, the overlapping contribution of these relaxation processes to $P_{1/2}$ data in the Orbach region cannot be accurately assessed.

On the other hand, the temperature dependence of $P_{1/2}$ data in the Raman region is not well-defined because of limitations in the incident microwave power of our spectrometer and the generally decreased signal-to-noise characteristics of samples at higher temperatures. For these reasons we have carefully compared[6,49] the temperature dependences of $P_{1/2}$ data of aquomethemoglobin, aquometmyoglobin, and metmyoglobin fluoride for which the zfs of the high-spin Fe^{3+} ion is defined through pulse saturation[51] and magnetic susceptibility[52] studies. On the basis of these comparitive studies, we conclude that the most accurate estimate of Δ in cw microwave saturation experiments is defined by $P_{1/2}$ data in the high-temperature portion of the central region adjacent to the break near $T \sim 10$ K that indicates the onset of the Raman process. In this manner, zfs estimates of 14, 22, and 12 cm^{-1} were obtained for these three hemeproteins, respectively, on the basis of $P_{1/2}$ data, in excellent agreement (±10%) with the results of magnetic susceptibility and pulse saturation and recovery experiments.[6] Therefore, we apply the same approach to the treatment of $P_{1/2}$ data of complexes of high-spin Co^{2+}.

In Figure 1, the linear portion of the graph yields an estimate of 6.6 cm^{-1} for Δ according to eq 4. In this equation, Δ is strictly

$$\frac{1}{T_1} = \frac{C(\Delta)^3}{\exp(\Delta/kT) - 1} \simeq C(\Delta)^3 \exp(-\Delta/kT) \quad (4)$$

defined[37-39] as the splitting between the lowest Kramers doublet and the lowest lying excited state, k is the Boltzmann constant, and C is a coefficient characteristic of the phonon–spin coupling properties of the matrix. For a Kramers ion with an excited spin doublet lying below the Debye limit, the value of Δ corresponds to the splitting between the two lowest Kramers doublets, in general, and is identical with the zfs in the case of a paramagnetic metal ion with an orbitally nondegenerate ground state.[37,38] Under the condition $\Delta >> kT >> h\nu$, the approximation in eq 4 can be straightforwardly applied.[53]

We have previously reported the EPR absorption spectrum of polycrystalline $Co_{0.001}Zn_{0.999}(imidazole)_2(acetate)_2$.[34,54] For this

(44) Rupp, H.; Rao, K. K.; Hall, D. O.; Cammack, R. *Biochim. Biophys. Acta* **1978**, *537*, 255–269.

(45) Blum, H.; Ohnishi, T. *Biochim. Biophys. Acta* **1980**, *621*, 9–18.

(46) Bloembergen et al.[47] have shown that under sufficiently intense modulation amplitude (H_m), T_2 in the saturation parameter is replaced by $1/\gamma H_m$. This latter condition implies a linear dependence of $P_{1/2}$ on H_m. For all of the complexes of Co^{2+} investigated here, we have observed that $P_{1/2}$ does not change within the 2–20 G modulation amplitude range under conditions of either 12.5 or 100-kHz microwave frequency modulation. Therefore, considerably more intense modulation fields must be used before application of eq 3 becomes invalid. We have observed a weak dependence of $P_{1/2}$ on H_m in the case of some high-spin Fe^{3+} hemeproteins;[6] however, the temperature dependence of $P_{1/2}$ determined at constant amplitude modulation still provides an accurate estimate of the zfs energy when compared to results of magnetic susceptibility or pulse saturation and recovery studies. Conditions of constant amplitude modulation have been invariably employed for each of the complexes investigated in this study.

(47) Bloembergen, N.; Purcell, E. M.; Pound, R. V. *Phys. Rev.* **1948**, *73*, 679–712.

(48) Abragam, A.; Bleaney, B. "Electron Paramagnetic Resonance of Transition Ions"; Clarendon Press: Oxford, **1970**; Chapter 10, pp 557–583.

(49) For these comparative experiments we have employed a pulse saturation and recovery spectrometer provided for our use by Professor H. J. Stapleton at the University of Illinois at Urbana since we are unable to achieve sufficiently low sample temperatures (< 2.5 K) to observe spin–lattice relaxation by the direct process only with the cryostat facilities in our laboratory.[6,33] Nonetheless, we have confirmed that estimates of Δ for high-spin Fe^{3+} complexes of hemeproteins originally determined by this cw saturation technique[6] are identical with those determined in pulse saturation and recovery[51] or in magnetic susceptibility[52] studies. Comparative studies could be carried out, however, only of high-spin Fe^{3+} hemeproteins because the klystron of the pulse saturation spectrometer was not sufficient to saturate the resonance absorption of high-spin Co^{2+} complexes at temperatures >2 K due to their significantly faster spin–lattice relaxation.

(50) (a) Portis, A. M. *Phys. Rev.* **1956**, *104*, 584–588. (b) Kiel, A. *Phys. Rev.* **1962**, *125*, 1451–1455. (c) Wolf, E. L. *Phys. Rev.* **1966**, *142*, 555–569.

(51) Scholes, C. P.; Isaacson, R. A.; Feher, G. *Biochim. Biophys. Acta* **1971**, *244*, 206–210.

(52) Uenoyama, H.; Iizuka, T.; Morimoto, H.; Kotani, M. *Biochim. Biophys. Acta* **1968**, *160*, 159–166.

(53) We have previously point out[6] that the application of the linear approximation in eq 4 leads to an overestimate of the zfs for values ≤10 cm^{-1}. This is not a serious error when considered with respect to the correlation of the value of Δ with coordination structure expressed in eq 1 and the three ranges of values of Δ identified for high-spin Co^{2+} in this study.

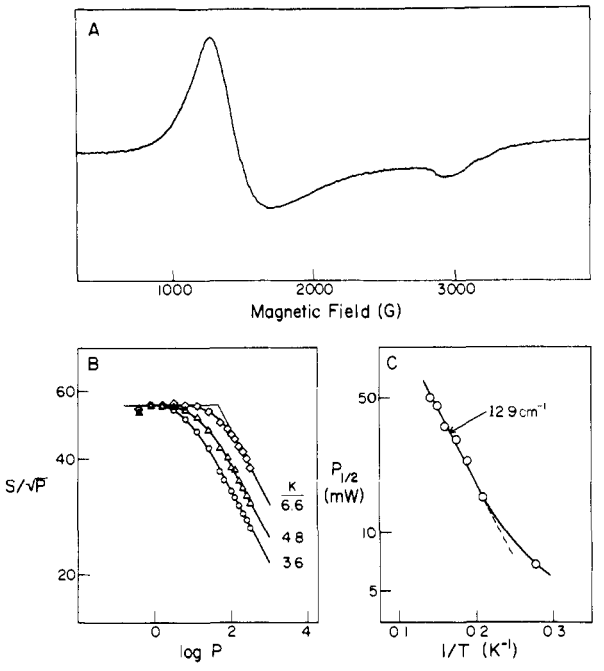

Figure 3. First-derivative EPR absorption spectrum and cw microwave power saturation properties of bis(triphenylphosphine)cobalt(II) chloride in frozen ethanol. The complex prepared in pure crystalline form was dissolved to a concentration of 5×10^{-4} M in absolute ethanol and frozen. (A) illustrates the spectrum recorded with the sample at 3.6 K with 63.7-mW incident microwave power and 8-G amplitude modulation. Other conditions as in Figure 2. Parallel experiments with solutions of $CoCl_2$ in ethanol at identical metal ion concentrations showed that the cw power saturation data could not be attributed to solvated high-spin Co^{2+}.

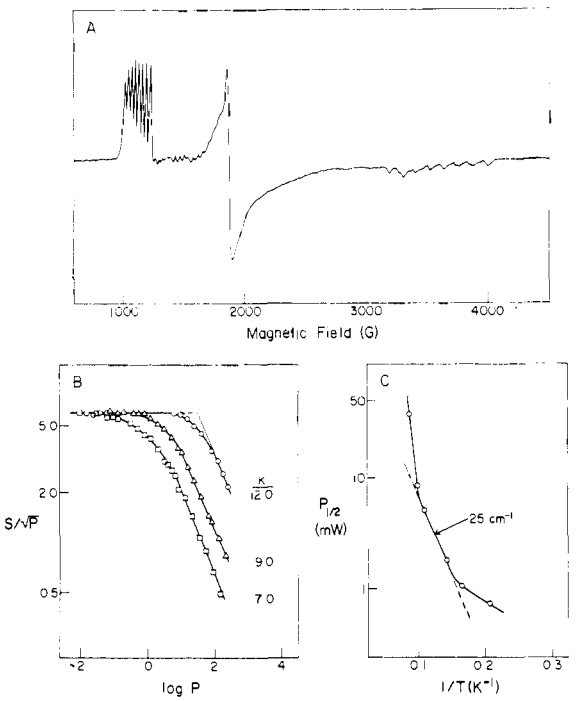

Figure 4. First-derivative EPR absorption spectrum and cw microwave saturation behavior of pentakis(2-picoline *N*-oxide)cobalt(II) perchlorate incorporated to ≤ 0.1 mol% into the polycrystalline matrix of the isomorphous[10] Zn^{2+} complex. (A) illustrates the spectrum recorded with the sample at 4.8 K with 0.8-mW incident microwave power and 6.3-G amplitude modulation. The resonance absorption features appear at g values of ~5.94, 3.56, and 1.91. Hyperfine structure resolved in both the $g \sim 5.94$ and $g \sim 1.91$ regions corresponds to an (average) coupling constant of 0.0081 cm^{-1} for the ($I = {}^7/_2$) ^{59}Co nucleus. (B) shows the cw microwave power dependence of the signal amplitude in the $g \sim 5.94$ region evaluated on the basis of the sum of the eight hyperfine components. For purposes of clarity, only the curves at 7.0, 9.0, and 12 K are shown. The slope at high values of P yields a value of −1.05 for b that remains temperature invariant over the 4–12 K range. (C) illustrates the temperature dependence of $P_{1/2}$.

compound we have estimated a value of 4.8 cm^{-1} for Δ by the cw microwave power technique (saturation curves not shown). Similarly we have observed that the value of Δ for the $(CoBr_4)^{2-}$ anion in frozen aqueous solution is 11.0 cm^{-1}.

In Figure 2 we have illustrated the EPR absorption spectrum of polycrystalline $Co_{0.002}Zn_{0.998}(Ph_3P)_2Cl_2$. The inset illustrates the saturation curvce of the absorption feature in the low-field region. In contrast to that in Figure 1, there is no distinct change in slope at high values of log P and the shape and position of the saturation curve do not change with temperature. For this polycrystalline material, we also observed that the peak-to-peak amplitude *increased* with increasing temperature at constant levels of incident (nonsaturating) microwave power until a maximum amplitude was observed at ~9 K. Comparable observations for other high-spin Co^{2+} systems have not been made in our previous investigations.[34-36] In Figure 3 is illustrated the EPR absorption spectrum of $Co(Ph_3P)_2Cl_2$ in a frozen ethanolic glass for the complex prepared by dissolving the organic ligand and $CoCl_2$ in strict 2:1 molar ratio. The inset illustrates the temperature dependence of $P_{1/2}$ plotted on the basis of the signal amplitude of the low-field portion of the $g \sim 4.6$ resonance feature. When excess organic ligand was added to the ethanolic solution, the peak-to-peak amplitude of the low-field absorption exhibited a time-dependent decrease in amplitude under conditions of high microwave power (>300 mW) irradiation. The time-dependent decrease in amplitude became more marked with increasing concentration of the organic ligand. In contrast, this phenomenon was not observed for the polycrystalline complex. In Figure 3C, the plot of $P_{1/2}$ vs. $1/T$ yields a value for Δ of 12.9 cm^{-1}. We shall discuss later the origin of the different saturation behavior of this complex in polycrystalline and solution states.

B. Pentacoordinate Complexes of High-Spin Co^{2+}. The first derivative EPR absorption spectrum of polycrystalline[11,12] $Co_{0.001}Zn_{0.999}$(2-picoline *N*-oxide)$_5(ClO_4)_2$ is shown in Figure 4. The spectrum is identical with that published by Bencini et al.[55]

In Figure 4C the temperature dependence of $P_{1/2}$, based on the sum of the signal amplitudes of the eight, low-field, hyperfine components centered at $g \sim 5.94$, yielded an estimate of 25.0 cm^{-1} for the value of Δ.

The EPR absorption spectrum of polycrystalline $Co_{0.002}Zn_{0.998}(MePh_2AsO)_4(ClO_4)_2$ is illustrated in Figure 5. The low-field region shows resolved hyperfine structure due to the ($I = {}^7/_2$) ^{59}Co nucleus centered at $g \sim 8.1$. The spectrum is essentially identical in line shape with that of the analogous nitrate complex.[56,57] We have also observed that the spectroscopic properties of the complex in frozen ethanolic solution are invariant under conditions of up to a 5-fold excess of the organic ligand. In Figure 5B the temperature dependence of $P_{1/2}$ evaluated for the $g \sim 3.0$ resonance feature of the polycrystalline complex is essentially indistinguishable from that for the complex in solution. In the high-temperature region near 10 K, $P_{1/2}$ data for the complex in solution yielded an estimate of 18.9 cm^{-1} for Δ. Experiments employing the analogous compound $Co(MePh_2PO)_4(ClO_4)_2$ in frozen solution yielded a value of 18.5 cm^{-1} for Δ.

(54) Kuo, L. C. Ph.D. Thesis, The University of Chicago, 1981, pp 306.

(55) Bencini, A.; Benelli, C.; Gatteschi, D.; Zanchini, C. *Inorg. Chem.* **1980**, *19*, 3839-3842.

(56) Bencini et al.[57] have reported that the EPR single-crystal spectrum of $Co(MePh_2AsO)_4(NO_3)_2$ incorporated into the host crystal matrix of the Zn^{2+} analogue is highly anisotropic with $g_1 \sim 8.6$, $g_2 \sim 1.3$, and $g_3 \sim 0.9$. Although these g-values differ from those of the polycrystalline perchlorate complex, the spectrum of the nitrate salt is essentially identical in shape. Although the nitrate and perchlorate complexes crystallize in the same space group,[18] it is not established by X-ray diffraction whether the two complexes are isostructural.

(57) Bencini, A.; Benelli, C.; Gatteschi, D.; Zanchini, C. *Inorg. Chem.* **1979**, *18*, 2526-2528.

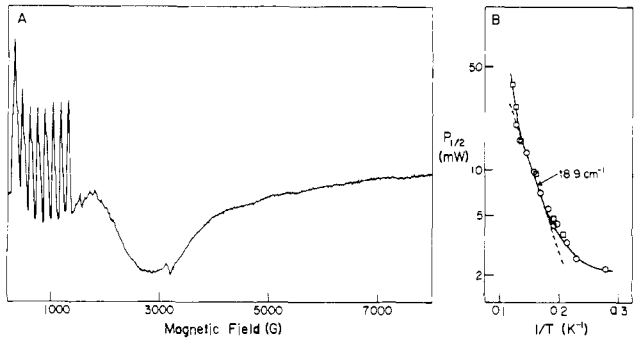

Figure 5. First-derivative EPR absorption spectrum and cw microwave saturation behavior of polycrystalline $Co_{0.002}Zn_{0.998}(MePh_2AsO)_4(ClO_4)_2$. The spectrum showing clearly resolved resonance features at $g \sim 8.1$ and 3.0 was recorded with the sample at 3.6 K and with 0.8-mW incident microwave power and 8-G amplitude modulation. The hyperfine structure resolved in the $g \sim 8.1$ region corresponds to an (average) coupling constant of 0.0529 cm^{-1} for the ^{59}Co nucleus. (B) compares the temperature dependence of $P_{1/2}$ of the polycrystalline sample (open squares) to that of the complex in solution illustrated as open circles. For the polycrystalline sample the microwave power saturation behavior is evaluated for the $g \sim 3.0$ resonance feature while that of the complex in solution is evaluated for the low-field component of the $g \sim 4.6$ resonance absorption feature of the solution spectrum. Although the respective $P_{1/2}$ values differ because of sample volumes and spin concentrations, the results from the two types of samples have been frame-shifted to illustrate the similar temperature dependences of $P_{1/2}$ in both polycrystalline and solution states. The value of 18.9 cm^{-1} is based on the data for the complex in solution near $T \sim 10$ K to minimize the contribution of relaxation processes at lower temperature due to spectral diffusion.

C. Hexacoordinate Complexes of High-Spin Co^{2+}. The structure of Co(pyridine *N*-oxide)$_6(ClO_4)_2$ exhibits perfect octahedral coordination geometry to within the estimated standard deviations of the X-ray defined atomic coordinates, and the cation sits in a site of S_6 symmetry.[24] Magnetic susceptibility measurements indicate, however, a trigonal field caused by a crystallographically undetectable elongation of the octahedron.[23,58] The lowest level of the high-spin Co^{2+} ion in this crystal has been assigned to $^4A_{1g}$ derived from the $^4T_1$ term in cubic symmetry, and a splitting of 53 cm^{-1} has been estimated between the two lowest levels of high-spin Co^{2+} in crystals of Co(pyridine *N*-oxide)$_6(ClO_4)_2$ on the basis of magnetic susceptibility studies.[58c]

In Figure 6 is illustrated the EPR absorption spectrum of Co(pyridine *N*-oxide)$_6(ClO_4)_2$ in frozen solution. The spectrum is consistent with the distortion described on the basis of magnetic susceptibility studies. Figure 6B shows a plot of the temperature dependence of $P_{1/2}$ for the low-field portion of the resonance feature at $g \sim 4.63$. The plot yields a value of 55 cm^{-1} for Δ. This is indicated as a lower limit only since the sharp increase in $P_{1/2}$ with temperature prevents observation of the onset of the Raman process expected near 10 K. This result is, nonetheless, in excellent agreement with the results of magnetic susceptibility studies.

We have similarly estimated that the values of Δ for polycrystalline $Co_{0.0005}Zn_{0.9995}SO_4 \cdot 7H_2O$, $Co_{0.0002}Mg_{0.9998}(acetate)_2 \cdot 4H_2O$, and $Co(Me_2SO)_6(ClO_4)_2$ in solution are ≥ 90, ~ 46, and ≥ 61 cm^{-1}, respectively.

Discussion

A. Determination of the Ground Term Splitting by Spin–Lattice Relaxation Dependent Processes. In this investigation we have included the complexes Cs_3CoBr_5[25] and $Co(Ph_3P)_2Cl_2$[19] because of the large, negative values of D determined for the Co^{2+} ion in pure, single crystals. For negative values of the zfs constant, the $m_s = \pm 3/2$ doublet is depressed relative to the $m_s = \pm 1/2$ doublet; however, the allowed EPR transitions can be observed only within

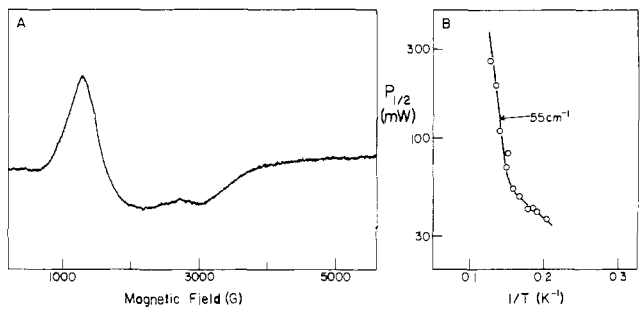

Figure 6. First-derivative EPR absorption spectrum and cw microwave power saturation behavior of hexakis(pyridine *N*-oxide)cobalt(II) perchlorate in frozen aqueous solution. For this spectrum $Co(ClO_4)_2$ was dissolved to a concentration of 3×10^{-4} M directly in the solvent in the presence of a 12:1 molar ratio of the organic ligand to the metal ion. The spin–lattice relaxation rate of the Co^{2+} ion increases rapidly above 5 K, a circumstance that limits the accuracy of determination of the value of $P_{1/2}$ with $\leq$640-mW incident microwave power. For this reason only a lower estimate of the value of Δ can be made by this cw microwave power saturation method.

the $m_s = \pm 1/2$ doublet when an X-band spectrometer is employed as in our investitgations. Under these conditions, application of the cw power saturation technique[6] monitors spin–lattice relaxation from the higher lying $m_s = \pm 1/2$ doublet which now corresponds to an excited state. We first demonstrate why conditions of large, negative values of D lead to an apparent value of 0 cm^{-1} for Δ when determined by the cw power saturation technique employed in this investigation and then discuss the importance of this result with respect to eq 1.

Orbach[37,59] has shown that the rate varies as $[\exp(\Delta/kT) - 1]^{-1}$ for spin–lattice relaxation from the lowest Kramers doublet (cf., eq 4) under the condition $\Delta >> kT >> h\nu$, and, therefore, an exponential dependence of the spin–lattice relaxation time on $1/T$ may be observed if the excited doublet lies below the Debye limit. On the other hand, for spin–lattice relaxation from the first excited doublet, Manenkov and Prokhorov[60] have shown that the spin–lattice relaxation rate varies as $[1 - \exp(-\Delta/kT)]^{-1}$. For spin–lattice relaxation according to the two-phonon (Orbach) resonance process, this condition leads to an essentially temperature-independent relaxation rate for values of $\Delta >> kT$. The temperature dependence of spin–lattice relaxation from the first excited Kramers doublet of Dy^{3+} doped into the host crystal of yttrium ethyl sulfate illustrates this relationship.[61] In this case, the value of Δ is ~ 14 cm^{-1}, and a flat curve describes the temperature dependence of $(1/T_1)$ in the 4–11 K range.

A large, negative value of D is assigned to the Co^{2+} ion in pure, single crystals of $Co(Ph_3P)_2Cl_2$.[19] The cw microwave saturation curves of polycrystalline $Co_{0.002}Zn_{0.998}(Ph_3P)_2Cl_2$ showed no clear change in slope at high values of log P and remained essentially temperature invariant, in contrast to other complexes employed in this investigation. Significantly, the peak-to-peak amplitude at constant (nonsaturating) microwave power increased with increasing temperature, indicating that the $m_s = \pm 1/2$ doublet is elevated with respect to the $m_s = \pm 3/2$ doublet, in confirmation of the results of magnetic susceptibility studies.[19] Our observation of maximum peak-to-peak amplitude at 9 K suggests an estimate of ~ -6 cm^{-1} for the value of Δ.

The spin–lattice relaxation behavior of $Co(Ph_3P)_2Cl_2$ in ethanolic solution differed greatly from that of the Co^{2+} ion in polycrystalline $Co_{0.002}Zn_{0.998}(Ph_3P)_2Cl_2$. We observed a time-dependent decrease in signal amplitude at high levels of incident microwave power with increasing concentration of the organic ligand in ethanol, a phenomenon not observed with polycrystalline samples. We suggest that this may be caused by aggregation of the complex due to the hydrophobic properties of the organic Ph_3P ligand in a hydrophilic solvent. On this basis, the spectroscopic

(58) (a) Mackey, D. J.; Evans, S. V. *J. Chem. Soc., Dalton Trans.* **1976**, 2004–2007. (b) Mackey, D. J.; McMeeking, R. F. *J. Chem. Soc., Dalton Trans.* **1977**, 2186–2189. (c) Mackey, D. J.; Evans, S. V.; McMeeking, R. F. *J. Chem. Soc., Dalton Trans.* **1978**, 160–165.

(59) Orbach, R. *Proc. Phys. Soc., London* **1961**, *77*, 821–826.

(60) Manenkov, A. A.; Prokhorov, A. M. *Sov. Phys.—JETP (Engl. Transl.)* **1962**, *15*, 951–953.

(61) Gill, J. C. *Proc. Phys. Soc., London* **1963**, *82*, 1066–1068.

properties of the complex in frozen solution in Figure 3 represent conditions of minimum perturbation since only a 2:1 molar ratio of the ligand and metal ion were employed. The results in Figure 3 show an exponential dependence of the relaxation rate with reciprocal temperature, indicating that the $m_s = \pm^1/_2$ doublet lies lowest for the complex in ethanolic solution and that, therefore, D is positive. Similarly the results for the tetrabromocobaltate(II) anion showed an exponential dependence of $P_{1/2}$ with reciprocal temperature, indicating that the $m_s = \pm^1/_2$ doublet also lies lowest for this complex in solution, in contrast to the results for crystals of Cs_3CoBr_5.[25]

We conclude that the structural distortions that result in large, negative values of D for $Co(Ph_3P)_2Cl_2$ and $(CoBr_4)^{2-}$ in the crystal imposed through molecular packing relationships are absent in solution. This conclusion implies that the predominant configuration of the ligands for each complex in solution is not precisely identical with that in crystals for which large, negative values of D obtain. This suggestion is supported on the basis of the angular overlap calculations of Horrocks and Burlone[62] who have identified the structural distortion in the $(CoCl_4)^{2-}$ anion that is responsible for the change in the value of $2D$ from -8.6 cm^{-1} in solid Cs_3CoCl_5[25] to $+9.3$ cm^{-1} in solid Cs_2CoCl_4.[26,27] The calculated change in structure increasing the value of $2D$ from -9 to $+9$ cm^{-1} is equivalent to an alteration of only $\sim 7°$ in the Cl–Co–Cl valence angle and is compatible with the X-ray defined structures of the $(CoCl_4)^{2-}$ anion in the two different crystal environments. Since both types of crystals are grown from aqueous solutions,[25-27] it is apparent that an equilibrium of the $(CoCl_4)^{2-}$ anion exists between two different ligand configurations. Similarly, an equilibrium between two ligand configurations of the $(CoBr_4)^{2-}$ anion must also obtain in aqueous solution, and our experimental conditions, i.e., freezing of the solution for EPR measurements, favors predominantly the structure associated with positive D. Just as the value of $2D$ changes for $(CoCl_4)^{2-}$ from $+9$ to -9 cm^{-1}, we observed a value of $2D$ of 11 cm^{-1} for one form of the $(CoBr_4)^{2-}$ anion, and in pure single crystals of Cs_3CoBr_5 the value of $2D$ is -10.6 cm^{-1}. It is likely that a similar equilibrium of ligand configurations obtains also for $Co(Ph_3P)_2Cl_2$.

We show later that a negative value of D can obtain only in distorted tetrahedral environments. Since this condition results in an apparent value of 0 cm^{-1} for Δ, when determined by the cw power saturation technique[6] employed here, this circumstance does not invalidate our correlation of the value of Δ with coordination geometry, as expressed through eq 1.

B. Dependence of the Splitting between the Two Lowest Kramers Doublets of High-Spin Co^{2+} on Spin–Orbit Coupling and Crystal Field Environment. The influence of spin–orbit coupling on the electronic properties of complex ions is discussed in numerous publications and monographs.[63-65] We consider, therefore, only those aspects that are necessary to establish the theoretical and quantitative correctness of the relationship expressed in eq 1 for high-spin Co^{2+}.

The splitting between the two lowest Kramers doublets of high-spin Co^{2+} is dependent on the strength of the crystal field, the relative magnitude of the distortion away from cubic symmetry, and the strength of the spin–orbit coupling. Under the conditions that the crystal field splittings are much greater than splittings induced by spin–orbit coupling, the energy separation of the levels split by spin–orbit interaction is given by the integral $\langle S\Gamma M_s a|\sum\xi\mathbf{l}_i\cdot\mathbf{s}_i|S\Gamma' M'_s a'\rangle$ where the spin–orbit interaction $V_{so} = \sum\xi\mathbf{l}_i\cdot\mathbf{s}_i$ is defined in terms of a dot product of $\mathbf{l}_i$, the orbital angular momentum operator, and $\mathbf{s}_i$, the spin angular momentum operator, of the ith electron, S is the spin quantum number, M_s is the z-component of the total angular momentum, and the orbital

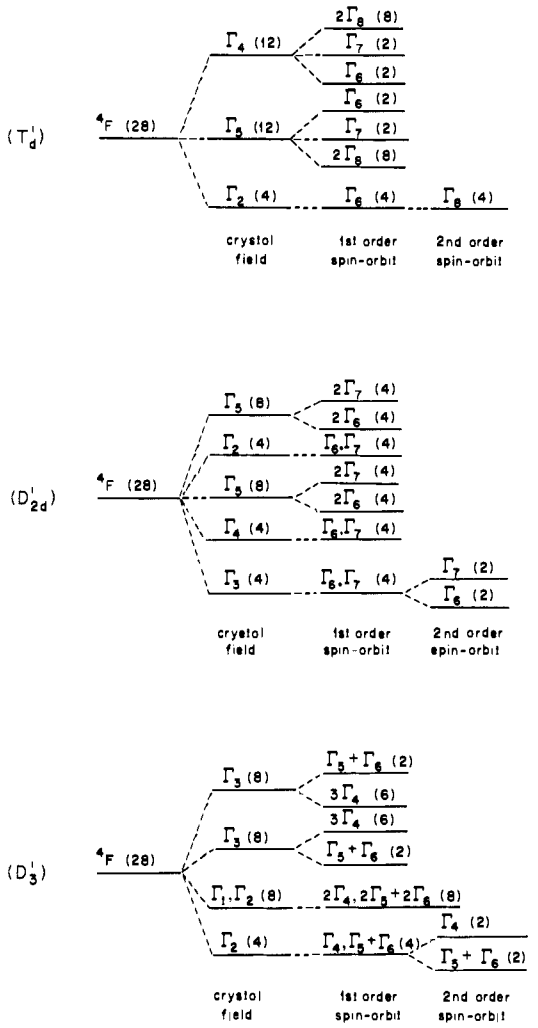

Figure 7. Term-splitting diagram of high-spin Co^{2+} in a crystal field of T'_d, D'_{2d}, and D'_3 symmetry (the prime indicates double point group notation). The multiplet splitting resulting from spin–orbit coupling is shown only for the ground state. The number in parentheses indicates the total spin and orbital degeneracies of each term. The upper part illustrates the splitting in T'_d symmetry; the central diagram corresponds to D'_{2d} symmetry, and the lower diagram corresponds to a site of D'_3 symmetry.

levels are defined by quantum numbers Γ and a. The symbol Γ is the irreducible representation of the orbit and a is a basis for this representation. In general, the summation over all electrons yields $V_{so} = \lambda\mathbf{L}\cdot\mathbf{S}$ where λ is the spin–orbit coupling constant and $\mathbf{L}$ and $\mathbf{S}$ are the orbital and spin angular momenta, respectively. This integral can be separated into the product of two integrals $\langle S\Gamma M_s a|\mathbf{l}_i|S\Gamma' M'_s a'\rangle\cdot\langle S\Gamma M_s a|\mathbf{s}_i|S\Gamma' M'_s a'\rangle$ wherein it is seen that the first integral is always zero unless the direct product of $\Gamma \times \Gamma_1 \times \Gamma$ contains the identity representation, Γ_1 being the irreducible representation of the orbital angular momentum. By group theoretical arguments, it can be shown for which orbital states this relationship obtains in a given crystal field environment.

In the upper part of Figure 7 is shown the term splitting diagram of the high-spin Co^{2+} ion in a crystal field of T'_d symmetry (the prime indicates double point group notation). In this environment, the ^4F state of the free, high-spin Co^{2+} ion is split into three levels that transform as $\Gamma_2(^4A_2)$, $\Gamma_5(^4T_2)$, and $\Gamma_4(^4T_1)$ where the degeneracy of the level is indicated in parentheses. The influence of spin–orbit coupling splits $\Gamma_5(^4T_2)$ and $\Gamma_4(^4T_1)$ each into three levels while the ground-state term $\Gamma_2(^4A_2)$ remains orbitally nondegenerate but now transforms as $\Gamma_8(^4A_2)$ because of the introduction of spin. The ground state $\Gamma_8(^4A_2)$ may interact by second-order spin–orbit coupling with $\Gamma_8(^4T_2)$ and $\Gamma_8(^4T_1)$. However, the overall 4-fold spin degeneracy of the ground state cannot be lifted by this interaction. Consequently, for a high-spin

(62) Horrocks, W. DeW., Jr.; Burlone, D. A. *J. Am. Chem. Soc.* **1976**, *98*, 6512–6516.
(63) Griffith, J. S. "The Theory of Transition Metal Ions"; Cambridge University Press: New York, 1961.
(64) Ballhausen, C. J. "Spin–Orbit Coupling"; McGraw-Hill: New York, 1962; Chapter VI, pp 113–151.
(65) Abragam, A.; Pryce, M. H. L. *Proc. R. Soc. London, Ser. A* **1951**, *206*, 173–191.

Table I. Summary of Spectroscopic Data of High-Spin Co^{2+} in Distorted Tetracoordinate Sites

host matrix	$2D_{obsd}$, cm^{-1}	$E(^4B_2)$, cm^{-1}		$E(^4E)$, cm^{-1}	$2\|D_{calcd}\|$,[a] cm^{-1}
Cs_3CoCl_5	−8.60[b]	3115[b]		2825[b]	7.6[c]
Cs_3CoBr_5	−10.68[b]				*d*
$[(CH_3)_4N)]_2ZnCl_4$	6.52[e]				*d*
Cs_2CoCl_4	9.3[f,g]				*d*
ZnO	5.50[h,i]	4400[j]		4100[j]	2.8
CdS	1.34[i,k]		3300[l]		0.8[m]
ZnS			3700[l]		1.2[m]
$Co(Ph_3P)_2Cl_2$	−6[n,o]		3500[p]		6.8[q]
yttrium gallium garnet	−36[o]	1795[r]		4000[s]	50.9
$PbWO_4$	9[t]		4000[u]		5.2[u]
$Zn[H_2B(pz)_2]_2$	0.8[t,v]				*d*

[a] Only the absolute value of $2D$ is calculated on the basis of eq 5, following the discussion by Jesson[66] who has shown that vibronic effects may obscure the assignment of the polarization of the excited states. For these estimates $\lambda = 0.8\lambda_0$ where λ_0 is the spin–orbit coupling constant for the free Co^{2+} ion (−178 cm^{-1} in ref 63). [b] Reference 25; also see discussion of these assignments by Jesson.[66] [c] Calculated on basis of the approximation $2D \sim -8\lambda^2\delta/(E_{mean})^2$ where $E_{mean} = [E(^4B_2) + E(^4E)]/2$, $\delta = |E(^4E) - E(^4B_2)|$, and δ is the orbital splitting of the $^4T_2(F)$ excited state, as discussed by Jesson.[66] A value of 800 cm^{-1} for the orbital splitting of the excited $^4T_2(F)$ state was used, as estimated by Jesson.[66] [d] Transition energies not reported. [e] Reference 67. [f] Reference 26. [g] Reference 27. [h] Reference 68. [i] Estimation by best fit of spin Hamiltonian parameters to EPR spectrum. [j] Estimation from polarized optical spectra in ref 69. [k] Reference 70. [l] Estimated as E_{mean} on the basis of polarized optical data in ref 71. [m] Estimated as in footnote *b*; in this case we have assumed a value for δ of 50 cm^{-1} on the basis of the discussion of the spectrum in ref 68. [n] For the complex dissolved in ethanol, we have determined a value of 12.9 cm^{-1}; the zfs of Co^{2+} in solid $Co(Ph_3P)_2Cl_2$ is reported[19] as large and negative, cf. discussion in text. [o] Estimated from EPR spectrum and temperature dependence of EPR absorption intensity as described in ref 72. [p] Estimated on the basis of the discussion of the polarized optical spectrum in ref 19. [q] Estimated as in footnote *b* with an orbital splitting of 500 cm^{-1}. [r] Provided as personal communication from D. L. Wood in ref 72. [s] Reference 73; also see ref 72. [t] Estimated on the basis of the temperature dependence of $P_{1/2}$ reported in ref 74; in that study, the authors have mistakenly assigned the Raman region to the Orbach process; we have corrected this error, keeping to the sequence of spin–lattice relaxation by Raman, Orbach, and direct processes in order of decreasing temperature.[48] [u] Estimate of E_{mean} made on the basis of the discussion of the polarized optical spectrum of $CoWO_4$ in ref 75; a value of $\delta = 500$ cm^{-1} is used as the orbital splitting of the $^4T_2(F)$ state. [v] Bis(dihydro)bis(1-pyrazolyl)boratozinc(II) served as the host matrix for the Co^{2+} analogue in EPR studies; structure determination and EPR studies reported in ref 76.

Co^{2+} ion in an environment of *exact* tetrahedral symmetry, the $m_s = \pm^3/_2$ and $m_s = \pm^1/_2$ components of the ground state are degenerate, and the value of the splitting between the two lowest Kramers doublets, which corresponds in this case directly to the zfs, is zero.

One common distortion of a Co^{2+} ion in a site of T'_d symmetry is a perturbation that lowers the symmetry to D'_{2d}. This is also illustrated in Figure 7. Correspondingly, the Γ_2, Γ_5, and Γ_4 terms in T'_d now transform as $\Gamma_3(^4B_1)$, $\Gamma_4(^4B_2) + \Gamma_5(^4E)$, and $\Gamma_2(^4A_2) + \Gamma_5(^4E)$, respectively. As a result of spin–orbit interaction, the ground state transforms as $\Gamma_6(^4B_1) + \Gamma_7(^4B_1)$. The $\Gamma_6 + \Gamma_7$ components of the orbitally nondegenerate ground state remain energetically equivalent in the absence of interactions with excited states. However, admixture of excited states through second-order spin–orbit coupling lifts the degeneracy of the $\Gamma_6 + \Gamma_7$ components of the ground state resulting in a nonzero value of the zfs energy. Accordingly, the sign of the zfs, i.e., $2D$, is determined by whether the $m_s = \pm^1/_2$ or $m_s = \pm^3/_2$ doublet lies lowest. By convention, the value of D is positive when the $m_s = \pm^1/_2$ doublet is lowest. On the basis of relationships derived[66] through second-order perturbation theory, the value of the zfs or $2D$ may be estimated according to eq 5 where $E(^4B_2)$ and $E(^4E)$ represent the crystal

$$2D = -8\lambda^2\left[\frac{1}{E(^4B_2)} - \frac{1}{E(^4E)}\right] \quad (5)$$

field transition energies to states derived from the excited $^4T_2(F)$ state. The crystal field transitions of high-spin Co^{2+} ion incorporated into a variety of distorted coordination sites of near T'_d symmetry have been identified through polarized absorption studies of single crystals. Moreover, for some of these systems the value of D has been estimated through magnetic susceptibility or EPR studies. The pertinent data are summarized in Table I. The experimentally determined values of $2D$ indicated under the heading $2D_{obsd}$ cover a wide range, but in general $2D < 13$ cm^{-1}. There is, furthermore, reasonable agreement between the experimentally observed magnitude of $2D$ and that calculated on the basis of eq 5 when appropriate correction for covalency is made on the basis of the spin–orbit coupling constant. Despite the large variety of chemically and structurally different environments represented in Table I, the magnitude of the zfs that results from second-order spin–orbit coupling is small for high-spin Co^{2+} in distorted tetracoordinate sites.

Table II. Summary of Spectroscopic Data of High-Spin Co^{2+} in Pentacoordinate Sites

compound	$E(^4E''(F))$,[a] cm^{-1}		$2D_{obsd}$, cm^{-1}	$2D_{calcd}$,[b] cm^{-1}
A. Trigonal Bipyramidal				
Co(2-picoline *N*-oxide)$_5$(ClO$_4$)$_2$[c]	5000[d]		25.0[e]	50
Co(Et$_4$dien)Br$_2$[f]	5000[g]			50
Co[Me$_6$tren)Cl]Cl[h]	5800[i]			43
Co(terpyridyl)Cl$_2$[j]	4800[k]			52
B. Square Pyramidal				
$Co(MePh_2AsO)_4(ClO_4)_2$[l]	5000[m,n]	6821[m,o]	18.9[e]	
$Co(MePh_2PO)_4(ClO_4)_2$[p]			18.5[e]	

[a] The range of reported values for the $^4A_2 \rightarrow {}^4E''(F)$ transition is 4800–7400 cm^{-1} in ref 28; here we present representative, classical structures. [b] Calculated on basis of eq 6 with $\lambda = 0.8\lambda_0$. [c] Structure defined in ref 11. [d] Reference 79. [e] This study. [f] Structure defined in ref 29; Et$_4$dien ≡ $[HNCH_2CH_2N(C_2H_5)_2]_2$. [g] Reference 30. [h] Structure defined in ref 32; Me$_6$tren ≡ $N[CH_2CH_2N(CH_3)_2]_3$. [i] Reference 80. [j] Structure defined in ref 31. [k] Reference 81. [l] Structure defined in ref 18. [m] Reference 82. [n] Transition energy for $^4A_2(F) \rightarrow {}^4B_2(F)$. [o] Transition energy for $^4A_2(F) \rightarrow {}^4E(F)$. [p] Probably isostructural with arsine oxide analogue.

Pentacoordinate Co^{2+} ions are found in complexes of square-pyramidal or trigonal-bipyramidal geometry. Here, we shall first restrict our discussion to the D'_3 point group. As shown in the lower part of Figure 7, spin–orbit coupling transforms the ground state into $\Gamma_4 + \Gamma_5 + \Gamma_6$ components and the excited states into $3\Gamma_4 + \Gamma_5 + \Gamma_6$. The degeneracy of the Γ_4 and $\Gamma_5 + \Gamma_6$ components of the ground state is lifted by second-order spin–orbit coupling interactions that mix excited-state terms into the ground state. The resultant effect is a nonzero value of the zfs even in the absence of distortion away from D'_3 symmetry. Essentially, a similar description obtains in C'_{3v} symmetry. In this case, the levels of the ground-state term also transform as Γ_4 and $\Gamma_5 + \Gamma_6$. However, the admixture of excited-state levels through spin-orbit coupling differs and, upon structural distortion, becomes dependent upon the angle that the equatorially directed metal–ligand bonds

(66) Jesson, J. P. *J. Chem. Phys.* **1968**, *48*, 161–168.
(67) McElearney, J. N.; Shankle, G. E.; Schwartz, R. W.; Carlin, R. L. *J. Chem. Phys.* **1972**, *56*, 3755–3758.
(68) Estle, T. L.; DeWit, M. *Bull. Am. Phys. Soc.* **1961**, *6*, 445.
(69) Papparlardo, R.; Wood, D. L.; Linares, Jr., R. C. *J. Chem. Phys.* **1961**, *35*, 2041–2059.
(70) Morigaki, K. *J. Phys. Soc. Jpn.* **1964**, *19*, 2064–2068.
(71) Weakliem, H. A. *J. Chem. Phys.* **1962**, *36*, 2117–2140.
(72) Sturge, M. D.; Merritt, F. R.; Hensel, J. C.; Remeika, J. P. *Phys. Rev.* **1969**, *180*, 402–412.
(73) Wood, D. L.; Remeika, J. P. *J. Chem. Phys.* **1967**, 46, 3595–3602.
(74) Chen, M. C.; Artman, J. O. *Phys. Rev.* **1969**, *187*, 723–732.
(75) Ferguson, J.; Wood, D. L.; Knox, K. *J. Chem. Phys.* **1963**, *39*, 881–889.
(76) Guggenberger, L. J.; Prewitt, C. T.; Meakin, P.; Trofimenko, S.; Jesson, J. P. *Inorg. Chem.* **1973**, *12*, 508–515.

make with the symmetry axis.[77] In both cases, however, the $m_s = \pm^1/_2$ Kramer doublet is lowest and only a positive value of the zfs is observed.

Wood[78] has evaluated the zfs of a high-spin d^7 ion with an orbitally nondegenerate ground state in a site of D'_{3h} symmetry and has shown that the zfs is approximated by eq 6 where the

$$2D = 12\lambda^2/E(^4E''(F)) \quad (6)$$

denominator term represents the $^4A'_2(F) \rightarrow {}^4E''(F)$ crystal field transition energy. In Table II we have summarized spectroscopic data that define the range of values of the zfs of high-spin Co^{2+} in pentacoordinate sites. Gatteschi and co-workers[28] have recently reviewed the paramagnetic properties of Co^{2+} in small molecule complexes. For the range of values reported for $E(^4E''(F))$, the value of Δ may range from 43 to 52 cm^{-1} on the basis of eq 6 for $\lambda = 0.8\lambda_0$. The experimentally determined value of 25 cm^{-1} for Co(2-picoline *N*-oxide)$_5$(ClO$_4$)$_2$, therefore, shows that the value of the spin–orbit coupling constant must be significantly decreased from the free ion value through covalency effects. Wood[78,83] has shown that lowering of the symmetry from D'_{3h} to C'_{3v} introduces an enhancement of the orbital contribution and that this derives from mixing of the $^4E''(F)$ excited state into the $^4A'_2$ ground state. For these reasons it seems that covalency effects are more important in pentacoordinate complexes than in tetracoordinate systems. Indeed, appropriate values of the covalency factor decreasing the spin–orbit coupling constant in pentacoordinate complexes of D_{3h} and C_{4v} symmetry have been estimated as 0.6–0.7.[84]

In the case of a pentacoordinate complex of Co^{2+} in C_{4v} symmetry with an orbitally nondegenerate ground state, relationships to estimate the zfs have not been explicitly derived comparable to eq 5 and 6. However, we can expect the sign of D to be positive for Co^{2+} in tetragonally distorted pentacoordinate sites. Griffith[85] has shown that the influence of a tetragonal field for a pentacoordinate site with a $^4A_2$ ground term is to depress the $m_s = \pm^1/_2$ doublet relative to the $m_s = \pm^3/_2$ doublet. In the case of the complex of Co(MePh$_2$AsO)$_4$(NO$_3$)$_2$, Gerloch and co-workers[82] have shown on the basis of polarized single-crystal absorption studies and angular overlap calculations that, of the three lowest terms, there is near degeneracy of $^4A_2(F)$ and $^4E(F)$ with $^4A_2(F)$ lowest. Mixing of the low-lying $^4E(F)$ excited state will markedly influence the splitting between the two lowest Kramers doublets, as in complexes of near D'_3 or C'_{3v} symmetry. Our estimate of the zfs of this complex (Table II), thus, shows it to be comparable in magnitude to that of high-spin Co^{2+} in pentacoordinate complexes of trigonal-bipyramidal geometry. No other data are reported in the literature to provide direct estimates of the splitting between the two lowest Kramers doublets in structurally defined, small molecule, pentacoordinate complexes of high-spin Co^{2+}.

For a high-spin Co^{2+} ion in a field of O' symmetry, the term scheme is the inverse of that for the T'_d point group illustrated in Figure 7. Since the ground state is orbitally 3-fold degenerate ($\Gamma_4(^4T_1)$), in contrast to all of the other cases discussed above, it is now associated with net orbital angular momentum. Distortion of the site may result in splitting of the $^4T_1$ ground state into an orbital singlet and an orbital doublet. With an orbitally degenerate ground state, there remains a significant unquenched orbital component and the splitting of the ground state does not correspond to a zfs, as defined by **S·D·S** for an orbitally nondegenerate term. Nonetheless, it is useful to discuss briefly the magnetic behavior of complexes with a signifant orbital component in order to differentiate them from tetra- and pentacoordinate complexes in which the orbital momentum is quenched.

Table III. Summary of Spectroscopic Data of High-Spin Co^{2+} in Hexacoordinate Sites

host matrix	g_1	g_2 or ($g_\perp$)	$g_\parallel$	g_3	Δ,[a] cm^{-1}
Mg(acetate)$_2$·4H$_2$O[b]	6.03[b]	3.89[b]		2.53[b]	~46[c]
Co(pyridine *N*-oxide)$_6$(ClO$_4$)$_2$[d]		4.63	2.27		≥55[c,e]
Co(Me$_2$SO)$_6$(ClO$_4$)$_2$[f]		4.63			≥61[c]
ZnSO$_4$·7H$_2$O[g]	7.11	2.91		2.83	≥90[c]
Al_2O_3					
site 1		4.95[h]	2.92[h]		110[i]
site 2		4.86[h]	2.81[h]		180[i]
MgF_2	5.84	4.12		2.14	152[j]
MgO		4.278[k,l]			305[k]
$CoCl_2$					275[m]

[a] Represents the splitting of the lowest two Kramers doublets derived from the $^4T_1$ ground state in cubic symmetry. [b] Reported in ref 14. [c] This study. [d] Structure defined in ref 24. [e] A calculated value of 53 cm^{-1} is reported in ref 58c by parametrization of an angular overlap model. [f] Structure defined in ref 21 and 22. [g] Structure discussed in ref 15 and 16. [h] Reference 86. [i] Splitting is determined on the basis of the temperature dependence of $P_{1/2}$ for Co^{2+} sites in corundum, as reported in ref 87. [j] Reference 88. [k] Reference 89. [l] An isotropic g value is determined in this case. [m] Reference 90.

The experimentally determined values of the splittings between the two lowest Kramers doublets of the ground state of high-spin Co^{2+} in hexacoordinate environments are summarized in Table III. As shown in the classical study by Low,[89] the three levels of the $^4T_1$ ground state of Co^{2+} in MgO corresponding to $m_J = \pm^1/_2, \pm^3/_2$, and $\pm^5/_2$ lie at energies $15\lambda/4$, $6\lambda/4$, and $-9\lambda/4$ (with respect to the undistorted $^4T_1$ level). In view of the analysis of Ham[91] indicating that the value of λ is not significantly reduced through Jahn–Teller distortions for Co^{2+} in MgO, we consider the value of 305 cm^{-1} as the approximate maximum upper limit for the splitting between the two lowest Kramers doublets of a Co^{2+} ion in a site of O' symmetry.[92] On the other hand, the splitting of 152 cm^{-1} between the lowest two doublets of the ^4E level arising from a tetragonal distortion of Co^{2+} in MgF_2 is due apparently to a rhombic component of approximately equal magnitude to the spin–orbit coupling.[88,93,94] The splittings of 110 and 180 cm^{-1} observed for the two Co^{2+} sites in Al_2O_3[86] are similarly interpreted[95] according to a distorted cubic field. In these sites of high-spin Co^{2+}, the orbital doublet of the trigonally split ground term is lowest. Analysis[58c] of the magnetic susceptibility data of Co(pyridine *N*-oxide)$_6$(ClO$_4$)$_2$ shows that the lowest level of the trigonally distorted $^4T_1$ level is the orbital singlet corresponding to $^4A_{1g}$ and that the two lowest Kramers doublets are separated by 53 cm^{-1}. In view of the similar splittings observed for Mg(Co)(acetate)$_2$·4H$_2$O, Co(Me$_2$SO)$_6$(ClO$_4$)$_2$, and Zn(Co)SO$_4$·7H$_2$O in this investigation, it is probable that these systems correspondingly have orbital singlets as the lowest level that derives from the $^4T_1$ ground state in a cubic environment.

C. Ground Term Splitting of High-Spin Co^{2+} as a Signature of Coordination Structure. The results of this study, together with the parameters summarized in Tables I–III, provide the most

(77) Bencini, A.; Gatteschi, D. *J. Phys. Chem.* **1976**, *80*, 2126–2132.
(78) Wood, J. S. *J. Chem. Soc. A* **1969**, 1582–1586.
(79) Bertini, I.; Dapporto, P.; Gatteschi, D.; Scozzafava, A. *Inorg. Chem.* **1975**, *14*, 1639–1643.
(80) Ciampolini, M.; Nardi, N. *Inorg. Chem.* **1966**, *5*, 41–44.
(81) Livingston, S. E.; Nolan, J. D. *J. Chem. Soc., Dalton Trans.* **1972**, 218–223.
(82) Gerloch, M.; Kohl, J.; Lewis, J.; Urland, W. *J. Chem. Soc.* **1970**, 3283–3296.
(83) (a) Wood, J. S. *Inorg. Chem.* **1968**, *7*, 852–859. (b) Wood, J. S.; Green, P. T. *Inorg. Chem.* **1969**, *8*, 491–497.
(84) Majumdar, D.; Ghosh, U. S. *Phys. Status Solidi B* **1972**, *49*, 91–100.
(85) Griffith, J. S. *Discuss. Faraday Soc.* **1958**, *26*, 81–86.
(86) Zverev, G. M.; Prokhorov, A. M. *Sov. Phys.—JETP (Engl. Transl.)* **1961**, *12*, 41–45.
(87) Zverev, G. M.; Petelina, N. G. *Sov. Phys.—JETP (Engl. Transl.)* **1962**, *15*, 820–823.
(88) Johnson, L. F.; Dietz, R. E.; Guggenheim, H. J. *Appl. Phys. Lett.* **1964**, *5*, 21–22
(89) Low, W. *Phys. Rev.* **1958**, *109*, 256–265.
(90) Hsu, E. C.; Stout, J. W. *J. Chem. Phys.* **1973**, *59*, 502–517.
(91) Ham, F. S. *Phys. Rev. A* **1965**, *138*, 1727–1740.
(92) The distortion from cubic symmetry for Co^{2+} in MgO is estimated[89] to be less than 10^{-3} cm^{-1}.
(93) Bates, C. A.; Wood, P. H. *Contemp. Phys.* **1975**, *16*, 547–560.
(94) Gladney, H. M. *Phys. Rev.* **1966**, *146*, 253–261.
(95) Rei, D. K. *Sov. Phys.—Solid State (Engl. Transl.)* **1962**, *3*, 1613–1626.

complete compilation of spectroscopic data hitherto that define the ground-state magnetic properties of high-spin Co^{2+} as a function of coordination geometry. The experimentally observed values of the zfs of high-spin Co^{2+} in distorted tetrahedral sites range from -36 to $+13$ cm^{-1}. The upper limit of 13 cm^{-1} coincides with the value of the zfs determined[36] for an inhibitor complex of active-site specific Co^{2+}-reconstituted liver alcohol dehydrogenase for which the distorted tetracoordinate environment of the metal ion is independently defined through X-ray crystallographic studies[96] at high resolution with phase refinement. Furthermore, in parallel studies we have determined that the value of Δ is 8.3 cm^{-1} in Co^{2+}-carboxypeptidase A[98] and 9.3 cm^{-1} for active site specific Co^{2+}-reconstituted liver alcohol dehydrogenase.[35] For both enzymes the active-site metal ion has been defined as tetraliganded on the basis of high-resolution, refined X-ray data.[100,101] In view of the large variety of inhibitor complexes of these Co^{2+}-substituted enzymes in which Δ has now been measured[35,36,97-99] and for which there is a large variation in ligand composition and metal–ligand bonding interactions, we conclude that a value of $+13$ cm^{-1} is the most probable maximum upper limit for Δ of high-spin Co^{2+} in distorted tetracoordinate sites.[104]

The range of values of the zfs of high-spin Co^{2+} in sites of pentacoordinate geometry is more difficult to define quantitatively because of the relative paucity of experimental observations. The two values of the zfs in Table II provided through this investigation and a value of 33 cm^{-1} determined by magnetic susceptibility studies of the acetazolamide inhibitor complex of Co^{2+}-reconstituted carbonic anhydrase[102a] (cf., also ref 35) are the only results in the literature for structurally defined pentacoordinate complexes. In parallel studies in this laboratory, we have determined zfs values of 39 cm^{-1} for the acylenzyme reaction intermediate of Co^{2+}-reconstituted carboxypeptidase A[54,98] and 30 cm^{-1} for the ternary enzyme–NAD^+–CF_3CH_2OH inhibitor complex of Co^{2+}-reconstituted liver alcohol dehydrogenase.[99] In both of these complexes we have confirmed pentacoordinate metal ion environments through enrichment of materials with ^{17}O.[34,106] Therefore, the results in Table II for high-spin Co^{2+} in sites of pentacoordinate geometry suggest that the values of $\sim$20 cm^{-1} are in the lower range expected and undoubtedly reflect the pronounced tendency[78,82,83] toward strong covalency in pentacoordinate environments. Our results, together with first-order estimates calculated by eq 6, indicate that the range of values of Δ of high-spin Co^{2+} in sites of pentacoordinate geometry with orbitally nondegenerate ground states may be expected to lie in the 20–50-cm^{-1} range. Furthermore, we note that in pentacoordinate complexes with axial symmetry, the $m_s = \pm^1/_2$ doublet lies lowest with D, therefore, positive, as derived through second-order perturbation theory.[78,85] Thus, the range for pentacoordinate complexes is nonoverlapping with that found for tetracoordinate sites. In parallel studies to define the coordination structure of Co^{2+}-reconstituted enzymes,[34-36,97-99] we have found considerable support through chemical and kinetic investigations to indicate that the coordination number of the active site metal ion is expanded to accommodate a fifth ligand in reaction intermediates. Thus, even an approximate value of Δ determined through spectroscopic studies becomes significant in assessing whether the coordination structure of the metal ion has been altered in the catalytic cycle because of the nonoverlapping range of values of Δ for Co^{2+} in tetra- and pentacoordinate sites.

The observed splittings of the two lowest Kramers doublets of high-spin Co^{2+} in orbitally degenerate ground states of hexacoordinate complexes, as shown in Table III, exhibit a range from 46 to 305 cm^{-1}. While this splitting does not correspond to a zfs as in complexes of high-spin Co^{2+} in an orbitally nondegenerate ground state, it can be measured directly by the temperature dependence of spin–lattice relaxation, as shown in this study, and in investigations by others.[87] The large splittings that are observed in these complexes are due to the influence of first-order spin–orbit coupling because of the unquenched orbital momentum. This classical problem has been treated in a number of textbooks and publications.[63-65] Although the range of the splittings for hexacoordinate Co^{2+} may overlap in part with that expected for the range of values of the zfs of Co^{2+} in pentacoordinate sites, they remain nonoverlapping with the range of values of $2D$ observed for tetracoordinate Co^{2+}.

Our conclusions find quantitative support through computational results according to theoretical models. Gatteschi and co-workers[28,37,57,77,103] have examined the influence of ligand composition and stereochemical distortion on the range of values of spin Hamiltonian parameters of the high-spin Co^{2+} ion according to angular overlap calculations. For tetracoordinate complexes with oxygen and nitrogen donor ligand environments of type CoA_2B_2 and $CoAB_3$, the value of $2D$ remains less than 20 cm^{-1} for $\lambda = 0.8\lambda_0$. Only in the special instance of a $CoAB_3$ complex in which three of the ligands each make an angle of 90–95° with the fourth axial ligand does the value of $2D$ become large and overlapping with the range calculated for pentacoordinate complexes. This latter, unusual condition is unlikely to obtain for any molecule in solution since the open site opposite the axial ligand would become occupied by a solvent molecule as the fifth ligand. Moreover, the results for high-spin pentacoordinate complexes with ligand environments of the type CoA_2B_3 and $CoAB_4$ yield only positive values for $2D$ in the 25–75-cm^{-1} range. Interestingly, only in the case of tetrahedral distortion of a pentacoordinate complex of trigonal-bipyramidal geometry, resulting in elongation of one of the axial bonds, does the calculated zfs energy of a pentacoordinate complex decrease significantly to overlap with the range calculated for tetracoordinate species.[103] The overlap commences when the ligand–Co–ligand valence angles formed with the four primary ligands has increased from 90° to 109°. This is precisely the condition in which *only* four donor-ligand atoms can be sterically accommodated in the inner coordination sphere of the metal ion. The calculated decrease in $2D$, thus, remains consistent with our correlation of the value of Δ with coordination number expressed in eq 1. These combined results, thus, support our conclusions that the splitting between the two lowest Kramers doublets of high-spin Co^{2+} is a direct spectroscopic signature of coordination structure.

Acknowledgment. We are indebted to Professors R. L. Carlin and J. W. Stout for helpful discussions on the theory of spin–orbit coupling and zero-field splitting. We also thank Professor Carlin for the gift of $Co(Ph_3P)_2Cl_2$.

Registry No. $Zn(Ph_3PO)_2Cl_2$, 14494-88-3; $Zn(imidazole)_2(acetate)_2$, 74194-01-7; $Zn(Ph_3P)_2Cl_2$, 14494-89-4; $Co(Ph_3P)_2Cl_2$, 14126-40-0; Zn(2-picoline *N*-oxide)$_5(ClO_4)_2$, 74763-42-1; $Zn(MePh_2AsO)_4(ClO_4)_2$, 97150-38-4; $Co(MePh_2PO)_4(ClO_4)_2$, 97150-40-8; Co(pyridine *N*-

(96) Cedergren-Zeppezauer, E.; Samama, J. P.; Eklund, H. *Biochemistry* **1982**, *21*, 4895–4908.
(97) Makinen, M. W.; Kuo, L. C.; Yim, M. B.; Maret, W.; Wells, G. B. *J. Mol. Catal.* **1984**, *23*, 179–186.
(98) Kuo, L. C.; Makinen, M. W. *J. Am. Chem. Soc.*, following paper in this issue.
(99) Yim, M. B.; Wells, G. B.; Maret, W.; Makinen, M. W., manuscript in preparation.
(100) Hardman, K.; Lipscomb, W. N. *J. Am. Chem. Soc.* **1984**, *106*, 463–464.
(101) Schneider, G.; Eklund, H.; Cedergren-Zeppezauer E.; Zeppezauer, M. *Proc. Natl. Acad. Sci. U.S.A.* **1983**, *80*, 5289–5293.
(102) (a) Aasa, R.; Hanson, M.; Lindskog, S. *Biochem. Biophys. Acta* **1976**, *453*, 211–217. (b) Kannan, K. K.; Vaara, I.; Notstrand, B.; Lövgren, S.; Borell, A.; Fridborg, K.; Petef, M. In "Drug Action at the Molecular Level"; Roberts, G. C. K., Ed.; University Park Press: Baltimore, MD; 1977, pp 73–91.
(103) Banci, L.; Bencini, A.; Benelli, C.; Gatteschi, D. *Nouv. J. Chim.* **1980**, *4*, 593–598.
(104) A referee has pointed out that the value of 23 cm^{-1} reported[105] for the zfs of tetracoordinate Co^{2+} in $[(n\text{-}C_4H_9)_4N][Co(C_9H_7N)Br_3]$ seemingly contradicts our assessment of the upper limit for Δ_4. The result reported by Gerloch and Hanton[105] is based on magnetic susceptibility data collected at temperatures higher than 25 K. As discussed by Carlin and van Duyneveldt,[4] the zfs must be measured under conditions where there are no thermally accessible states whose populations change significantly with changing temperature. This stipulation requires that $T < |D|$ for valid estimates of the zfs by magnetic susceptibility methods.
(105) Gerloch, M.; Hanton, L. R. *Inorg. Chem.* **1980**, *19*, 1692–1698.
(106) Yim, M. B.; Wells, G. B.; Kuo, L. C.; Makinen, M. W. In "Bioinorganic Chemistry 85"; Xavier, A. V., Ed.; VCH Verlagsgesellschaft: Weinheim, FRG, 1985, in press.

oxide)$_6$(ClO$_4$)$_2$, 18533-53-4; ZnSO$_4$, 7733-02-0; Mg(acetate)$_2$, 142-72-3; Co(Me$_2$SO)$_6$(ClO$_4$)$_2$, 15553-90-9; Co(2-picoline *N*-oxide)$_5$(ClO$_4$)$_2$, 21460-56-0; Co(MePh$_2$AsO)$_4$(NO$_3$)$_2$, 97150-41-9; Cs$_3$CoCl$_5$, 13774-14-6; Cs$_3$CoBr$_5$, 13826-97-6; [(CH$_3$)$_4$N]$_2$ZnCl$_4$, 14240-97-2; Cs$_2$CoCl$_4$, 15007-14-4; ZnO, 1314-13-2; CdS, 1306-23-6; ZnS, 1314-98-3; PbWO$_4$, 12737-98-3; Zn[H$_2$B(pz)$_2$]$_2$, 18131-19-6; Co(Et$_4$dien)Br$_2$, 20506-81-4; Co[(Me$_6$tren)Cl]Cl, 97150-42-0; Co(terpyridyl)Cl$_2$, 14854-50-3; Co(MePh$_2$AsO)$_4$(ClO$_4$)$_2$, 18712-83-9; ZnSO$_4$, 7733-02-0; Al$_2$O$_3$, 1344-28-1; MgF$_2$, 7783-40-6; MgO, 1309-48-4; CoCl$_2$, 7646-79-9; Co, 7440-48-4; yttrium gallium garnet, 12024-41-8.

Ground Term Splitting of High-Spin Co^{2+} as a Probe of Coordination Structure. 2. The Ligand Environment of the Active Site Metal Ion of Carboxypeptidase A in Ester Hydrolysis[1a]

Lawrence C. Kuo[1b] and Marvin W. Makinen*[1c]

Contribution from the Department of Biophysics and Theoretical Biology, The University of Chicago, Cummings Life Science Center, Chicago, Illinois 60637. *Received April 9, 1984*

Abstract: The value of the zero-field splitting of Co^{2+}-substituted carboxypeptidase A is employed to assign the coordination structure of the active-site metal ion. The zero-field splitting of the Co^{2+} ion is 8.3 cm^{-1} in the free enzyme, 51 cm^{-1} in the enzyme–L-benzylsuccinate inhibitor complex, and 39 cm^{-1} for the mixed anhydride reaction intermediate formed with *O*-(*trans*-*p*-chlorocinnamoyl)-L-β-phenyllactate and stabilized by cryoenzymologic techniques. The value of 8.3 cm^{-1} is compatible only with a distorted tetraliganded complex while the value of 39 cm^{-1} for the acylenzyme reaction intermediate can be accounted for only by a pentaliganded active-site metal ion. Together with previous results of electron paramagnetic resonance experiments with use of ^{17}O-enriched substrate or solvent (Kuo, L. C.; Makinen, M. W. *J. Biol. Chem.* **1982**, *257*, 24–27], the results demonstrate that the coordination number of the metal ion in the free enzyme is increased in the mixed anhydride intermediate to accommodate both a water molecule and the carbonyl oxygen of the scissile bond of the substrate, in addition to the three ligands from protein residues. The mechanism of carboxypeptidase A in esterolysis is reevaluated in light of these findings, and criteria for accumulation of the reaction intermediate by cryoenzymologic methods for structural characterization are discussed.

Enzymes catalyze reactions via the sequential formation of a series of reaction intermediates. An important objective to understand the basis of enzyme function is to determine the structures of reaction intermediates. One means to achieve this goal is through application of an integrated, multidisciplinary approach employing cryoenzymologic techniques[2–4] with kinetic and structural methods. By use of cryoenzymologic methods, we have demonstrated that in the esterolytic reaction catalyzed by carboxypeptidase A an acylenzyme (mixed anhydride) reaction intermediate is formed with the specific ester substrate *O*-(*p*-chlorocinnamoyl)-L-β-phenyllactate.[5–9] A salient result of these investigations, in contrast to the implications of structural studies of inhibitor complexes,[10–13] is that the water molecule coordinated to the metal ion is not displaced by the substrate in the mixed anhydride intermediate.[6] These results imply that the tetraligand coordination environment of the active-site metal ion in the free enzyme[10–13] is altered to accommodate a fifth ligand in the course of the reaction. An important objective in structural studies of this enzyme, therefore, is to assign directly the coordination environment of the active-site metal ion in the acylenzyme (mixed anhydride) reaction intermediate.

Our kinetic and cryoenzymologic studies reveal that the mechanism of ester hydrolysis is identical for both native Zn^{2+}-containing and Co^{2+}-reconstituted carboxypeptidase A and that on this basis the paramagnetic Co^{2+} ion may serve as a direct spectroscopic probe of catalytically required structural relationships in the active site. To determine the ligand environment of the active-site metal ion in the acylenzyme reaction intermediate, we have carried out a detailed evaluation of the spectroscopic properties of high-spin Co^{2+}.[14–16] On the basis of these results, we

(1) (a) This work was supported by NIH Grant GM 21900. (b) Supported as a predoctoral student by a training grant of the NIH (GM 07183). Present address: Department of Chemistry, Boston University, Boston, MA 02215. (c) Established Investigator of The American Heart Association for part of the tenure of this investigation.

(2) Douzou, P. "Cryobiochemistry"; Academic Press: New York, 1977.

(3) Makinen, M. W.; Fink, A. L. *Annu. Rev. Biophys. Bioeng.* **1977**, *6*, 301–343.

(4) Fink, A. L.; Cartwright, S. J. *CRC Crit. Biochem.* **1981**, *11*, 145–207.

(5) Makinen, M. W.; Kuo, L. C.; Dymowski, J. J. Jaffer, S. *J. Biol. Chem.* **1979**, *254*, 356–366.

(6) Kuo, L. C.; Makinen, M. W. *J. Biol. Chem.* **1982**, *257*, 24–27.

(7) Kuo, L. C.; Fukuyama, J. M.; Makinen, M. W. *J. Mol. Biol.* **1982**, *163*, 63–105.

(8) Makinen, M. W.; Fukuyama, J. M.; Kuo, L. C. *J. Am. Chem. Soc.* **1982**, *104*, 2667–2669.

(9) Makinen, M. W.; Yamamura, K.; Kaiser, E. T. *Proc. Natl. Acad. Sci. U.S.A.* **1976**, *73*, 3882–3886.

(10) (a) Quiocho, F. A.; Lipscomb, W. N. *Adv. Protein Chem.* **1971**, *25*, 1–78. (b) Hartsuck, J. A.; Lipscomb, W. N. "The Enzymes"; Boyer, P. D., Ed.; Academic Press: New York, 1971; Vol. III, pp 1–56.

(11) (a) Rees, D. C.; Lewis, M.; Honzatko, R. B.; Lipscomb, W. N.; Hardman, K. D. *Proc. Natl. Acad. Sci. U.S.A.* **1981**, *78*, 3408–3412. (b) Rees, D. C.; Lewis, M.; Lipscomb, W. N. *J. Mol. Biol.* **1983**, *168*, 367–387.

(12) Lipscomb, W. N. *Tetrahedron* **1974**, *30*, 1725–1732.

(13) Lipscomb, W. N. *Acc. Chem. Res.* **1982**, *15*, 232–238.

(14) Makinen, M. W.; Yim, M. B. *Proc. Natl. Acad. Sci. U.S.A.* **1981**, *78*, 6221–6225.

(15) Makinen, M. W.; Kuo, L. C.; Yim, M. B.; Maret, W.; Wells, G. B. *J. Mol. Catal.* **1984**, *23*, 179–186.

(16) Makinen, M. W.; Kuo, L. C.; Yim, M. B.; Wells, G. B.; Fukuyama, J. M.; Kim, J. E. *J. Am. Chem. Soc.*, preceding paper in this issue.

0002-7863/85/1507-5255$01.50/0